

Climate-driven zooplankton shifts cause large-scale declines in food quality for fish

Received: 2 October 2021

Accepted: 13 February 2023

Published online: 23 March 2023

 Check for updates

Ryan F. Heneghan¹✉, Jason D. Everett^{2,3,4}, Julia L. Blanchard⁵,
Patrick Sykes² & Anthony J. Richardson^{2,3}

Zooplankton are the primary energy pathway from phytoplankton to fish. Yet, there is limited understanding about how climate change will modify zooplankton communities and the implications for marine food webs globally. Using a trait-based marine ecosystem model resolving key zooplankton groups, we find that future oceans, particularly in tropical regions, favour food webs increasingly dominated by carnivorous (chaetognaths, jellyfish and carnivorous copepods) and gelatinous filter-feeding zooplankton (larvaceans and salps) at the expense of omnivorous copepods and euphausiids. By providing a direct energetic pathway from small phytoplankton to fish, the rise of gelatinous filter feeders partially offsets the increase in trophic steps between primary producers and fish from declining phytoplankton biomass and increases in carnivorous zooplankton. However, future fish communities experience reduced carrying capacity from falling phytoplankton biomass and less nutritious food as environmental conditions increasingly favour gelatinous zooplankton, slightly exacerbating projected declines in small pelagic fish biomass in tropical regions by 2100.

Zooplankton are a critical component of marine food webs, serving as the primary energy pathway from phytoplankton to fish¹. Zooplankton are extremely diverse, representing 15 phyla² and accounting for ~40% of the world's marine biomass³. However, despite their abundance and ecological importance, most ecosystem models resolve few zooplankton groups⁴, focusing on phytoplankton or fish, particularly in climate change projections^{5,6}. By not adequately resolving zooplankton communities in ecosystem models, major climate-driven changes in marine food webs in response to climate change may be overlooked^{7–9}. These changes could have important implications for ecosystem services ranging from biogeochemical cycling^{10–12} to fisheries^{1,13}.

Zooplankton community structure across space and time is determined by how the vastly different functional traits of its members drive interactions between individual zooplankton and their environment^{8,14}. Zooplankton functional traits not only govern

the relative fitness of individual zooplankton^{7,8,15} but also regulate the transfer of energy from phytoplankton to fish^{8,14,15}. For example, the number of trophic steps between phytoplankton and fish is partly determined by zooplankton predator–prey mass ratios (PPMRs; the ratio of predator–prey body size). Higher PPMRs mean fewer trophic steps and therefore less energy lost from phytoplankton to fish¹⁶. Thus, communities dominated by carnivorous copepods (PPMR < 100; Supplementary Table 1) are expected to transfer less energy to higher trophic levels than those dominated by filter feeders such as larvaceans and salps¹⁶ (PPMR > 6 million; Supplementary Table 1). Zooplankton community composition also affects the nutritional quality (carbon content) of food for fish. This is because zooplankton carbon content varies within taxa and by over one order of magnitude across taxa¹⁷, from gelatinous zooplankton (0.5%), through crustaceans (12%), to microzooplankton (15%). Better accounting for

¹School of Mathematical Sciences, Queensland University of Technology, Brisbane, Queensland, Australia. ²School of Mathematics and Physics, The University of Queensland, St. Lucia, Queensland, Australia. ³Commonwealth Scientific and Industrial Research Organisation (CSIRO) Environment, Queensland Biosciences Precinct, St Lucia, Queensland, Australia. ⁴Centre for Marine Science and Innovation, School of Biological, Earth and Environmental Sciences, University of New South Wales, Sydney, New South Wales, Australia. ⁵Institute for Marine and Antarctic Studies, University of Tasmania, Hobart, Tasmania, Australia. ✉e-mail: ryan.heneghan@gmail.com

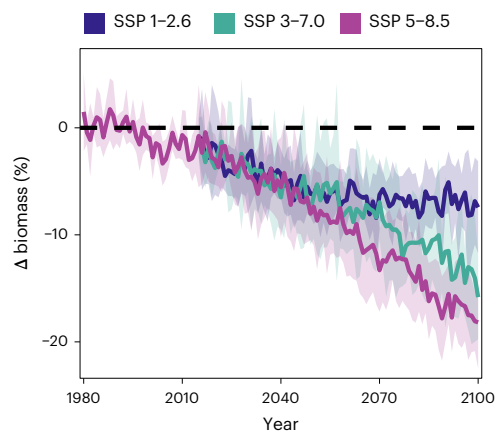


Fig. 1 | Effects of climate change on global zooplankton biomass. Change in global zooplankton biomass (%) for three zooplankton groups from 1980 to 2100, relative to 1980 to 2000, under emission scenarios SSP 1–2.6, SSP 3–7.0 and SSP 5–8.5. Solid lines represent the ensemble mean change in zooplankton biomass and shaded areas are the standard deviation from separate simulations of ZooMSS, each forced by one of five Earth-system models. The horizontal black dashed line indicates no change in biomass, compared to mean biomass in 1980–2000.

the diversity of zooplankton functional traits will therefore improve understanding of energy flow from plankton to fish now and under future climate change.

In this Article, we assess effects of climate change on global zooplankton community composition. We then explore how these climate-driven changes affect small pelagic (planktivorous) fish—the primary predator of zooplankton beyond zooplankton themselves. We use a global marine ecosystem model, the Zooplankton Model of Size Spectra (ZooMSS)¹⁸ (Methods), which resolves phytoplankton, two microzooplankton groups (heterotrophic flagellates and ciliates), seven mesozooplankton and macrozooplankton groups (omnivorous and carnivorous copepods, larvaceans, euphausiids, salps, chaetognaths and jellyfish) and three size-based fish groups (broadly representing small pelagic fish (SPF) ≤ 100 g; medium pelagic fish 100 g ≤ 10 kg and large pelagic fish 10 kg ≤ 1 t). ZooMSS resolves the nine zooplankton groups on the basis of several traits: the size range of the group, feeding characteristics (PPMR and feeding kernel width) and carbon content¹⁸ (Supplementary Table 1). We focus our analysis on the mesozooplankton and macrozooplankton (hereafter called zooplankton), organizing them into three groups defined by their feeding characteristics—carnivores (chaetognaths, jellyfish and carnivorous copepods), omnivores (euphausiids and omnivorous copepods) and filter feeders (larvaceans and salps). ZooMSS is forced by sea-surface temperature and phytoplankton variables from five coupled model intercomparison project phase 6 (CMIP6) Earth-system models¹⁹ under three future (2015–2100) Intergovernmental Panel on Climate Change shared socioeconomic pathways (SSPs)²⁰ (SSP 1–2.6, SSP 3–7.0 and SSP 5–8.5) using historical (1980–2014) conditions as a baseline (Methods).

Climate-driven declines in global zooplankton biomass

Global zooplankton biomass declined by 7–16% from 1980 to 2100 (Fig. 1 and Table 1). These declines in zooplankton biomass are within the range of similar studies^{21,22} and are primarily caused by projected declines in phytoplankton biomass. Of course, ZooMSS could be within range of other models for the wrong reasons or due to compensation effects (section on Model caveats). Contemporary distributions of zooplankton and small fish biomass at the global

level and their future declines show similar spatial and temporal patterns to phytoplankton biomass (Extended Data Fig. 1). This is because in ZooMSS phytoplankton are the primary food source for microzooplankton²³, filter feeders²⁴ and omnivorous zooplankton²⁵, which are themselves food for carnivores and SPF^{26–28} (Extended Data Fig. 2). Therefore, a decline in phytoplankton means less zooplankton and fish can be supported. Previous modelling and observational studies have also shown that contemporary and future zooplankton biomass is strongly related to phytoplankton biomass over large spatial scales^{21,22,29}. Warming acts as an additional driver of biomass decline in ZooMSS by increasing background mortality from senescence, which is not balanced by predation-driven growth. However, since predation-driven growth and mortality processes scale in the same way with temperature across all functional groups in ZooMSS (section on The model), warming is a secondary driver of zooplankton and fish biomass decline compared to decreases in phytoplankton biomass^{18,30}.

The decline in global biomass (from 1980 to 2100) varied across zooplankton groups (Fig. 2a–c and Table 1). Omnivorous zooplankton biomass exhibited the greatest decline of 8–18%. By contrast, filter feeders experienced a more modest biomass decline of up to 6%. The magnitude of decline of carnivorous zooplankton biomass was even less than filter feeders, decreasing between 1% and 2%. The greater decline in omnivores is a consequence of the relatively greater projected global reductions in nanophytoplankton (2–20 μm) and microphytoplankton (>20 μm) biomass under climate change—both major components of omnivore diets (Extended Data Fig. 2i,k)—in comparison to smaller picophytoplankton (<2 μm)^{8,14} (Extended Data Fig. 3a–c).

There was considerable variation in the response of each zooplankton group across ocean biomes (Fig. 2d–l and Table 1). From 1980 to 2100, omnivore biomass declined $>25\%$ under both SSP 3–7.0 and SSP 5–8.5 in tropical areas. By contrast, filter-feeder biomass was the least affected by climate change, varying between an increase of 2% in the polar biome (SSP 3–7.0, SSP 5–8.5) and a decrease of 8% in tropical waters (SSP 5–8.5). The magnitude of the change for carnivores was even smaller than filter feeders, with changes varying between a decline of 4% in polar regions under SSP 3–7.0 and SSP 5–8.5 and no change in tropical waters under SSP 1–2.6.

Climate-driven shifts in global zooplankton composition

Biomass declines across the zooplankton groups manifest spatially as disparate shifts in the composition of the zooplankton community (Fig. 3). Under historical (1980–2000) conditions, carnivorous and filter-feeding zooplankton constitute up to 50% of zooplankton in oligotrophic subtropical gyres (Fig. 3a,b) where phytoplankton and zooplankton biomass is lower^{31,32} (Extended Data Fig. 1a,b) and picophytoplankton—a major component in the diets of microzooplankton and filter feeders (Extended Data Fig. 2a,c,e,g)—dominate (Extended Data Fig. 4a). By contrast, omnivorous zooplankton constitute 60–90% of zooplankton biomass in polar and upwelling regions (Fig. 3c) where phytoplankton and zooplankton biomass are higher and nanophytoplankton and microphytoplankton are prevalent^{31,32} (Extended Data Fig. 4b,c).

Carnivorous and gelatinous filter-feeding zooplankton increase in dominance with climate change, particularly in expanding open-ocean oligotrophic gyres (Fig. 3d–l), with the magnitude of changes increasing with greater future emissions. Under SSP 1–2.6, carnivorous and filter-feeding zooplankton each increased as a proportion of zooplankton biomass by up to 10% across large areas. Omnivorous zooplankton declined by $>15\%$ as a proportion of total zooplankton biomass under all emission scenarios, in areas where the relative prevalence of carnivores and filter feeders increased. Within the three groups, patterns of change in individual zooplankton groups were broadly similar (Supplementary Figs. 1d–l, 2c–h and 3c–h).

Table 1 | Changes in global zooplankton under climate change

	Total zooplankton			Carnivores			Filter feeders			Omnivores		
	SSP1-2.6	SSP3-7.0	SSP5-8.5	SSP1-2.6	SSP3-7.0	SSP5-8.5	SSP1-2.6	SSP3-7.0	SSP5-8.5	SSP1-2.6	SSP3-7.0	SSP5-8.5
Global	-7±3***	-12±5***	-16±4***	-1±2**	-2±5*	-2±6*	-1±2***	-5±4***	-6±5***	-8±4***	-14±5***	-18±4***
Polar	-8±10***	-5±7***	-8±11***	-3±4***	-4±5***	-4±5***	2±3***	1±2	0±2	-8±11***	-5±8***	-8±13***
Temperate	-5±3***	-7±7***	-11±5***	-1±1***	-1±2***	-2±3***	-1±2**	-4±3***	-5±3***	-5±3***	-8±8***	-12±5***
Tropical	-9±6***	-22±10***	-27±10***	0±3	-2±8	-2±10*	-3±3***	-7±7***	-8±8***	-12±8***	-28±12***	-34±11***

Mean (±standard deviation) biomass change (%) in 2080 to 2100, relative to the mean over 1980–2000, for total zooplankton, carnivores (chaetognaths, jellyfish and carnivorous copepods), filter feeders (larvaceans and salps) and omnivores (euphausiids and omnivorous copepods) across SSPs and biomes. Note here that temperate and tropical, respectively, correspond to westerlies and trades Longhurst biomes and global results exclude the coastal biome (Extended Data Fig. 10 provides a map of the biomes). Each mean and standard deviation is calculated over five model simulations, with each simulation using a different Earth-system model to provide environmental forcings. *P* values from two-sided Mann–Whitney non-parametric *U*-tests comparing initial (1980–2000, *n*=100; 20 years×5 simulations) and final (2080–2100, *n*=100) biomass change are summarized as: *0.01 < *P* ≤ 0.05, **0.001 < *P* ≤ 0.01 and ****P* ≤ 0.001.

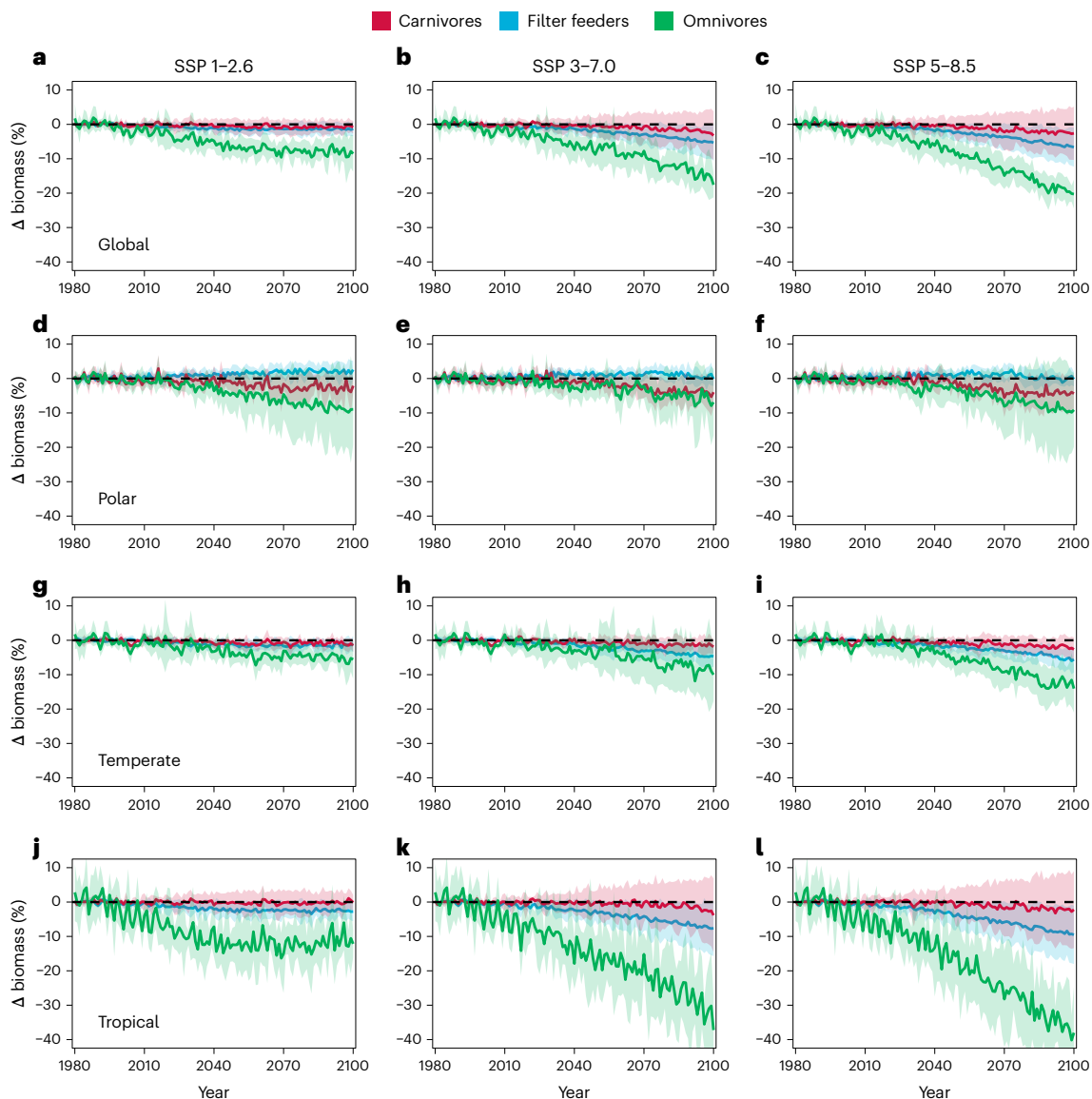


Fig. 2 | Effects of climate change on major zooplankton groups. a–l, Change in biomass (%) for three zooplankton groups (carnivores, filter feeders and omnivores) from 1980 to 2100, relative to 1980 to 2000, under emission scenarios SSP 1–2.6 (a,d,g,j), SSP 3–7.0 (b,e,h,k) and SSP 5–8.5 (c,f,i,l), across global (a–c), polar (d–f), temperate (g–i) and tropical (j–l) waters. Note here that temperate and tropical, respectively, correspond to westerlies and trades

Longhurst biomes and global results exclude the coastal biome; Extended Data Fig. 10 gives a map of the biomes. Solid lines represent the ensemble mean change in zooplankton biomass and shaded areas are the standard deviation from separate simulations of ZooMSS, each forced by one of five Earth-system models. The dashed black line in each plot represents no change from mean biomass in 1980–2000.

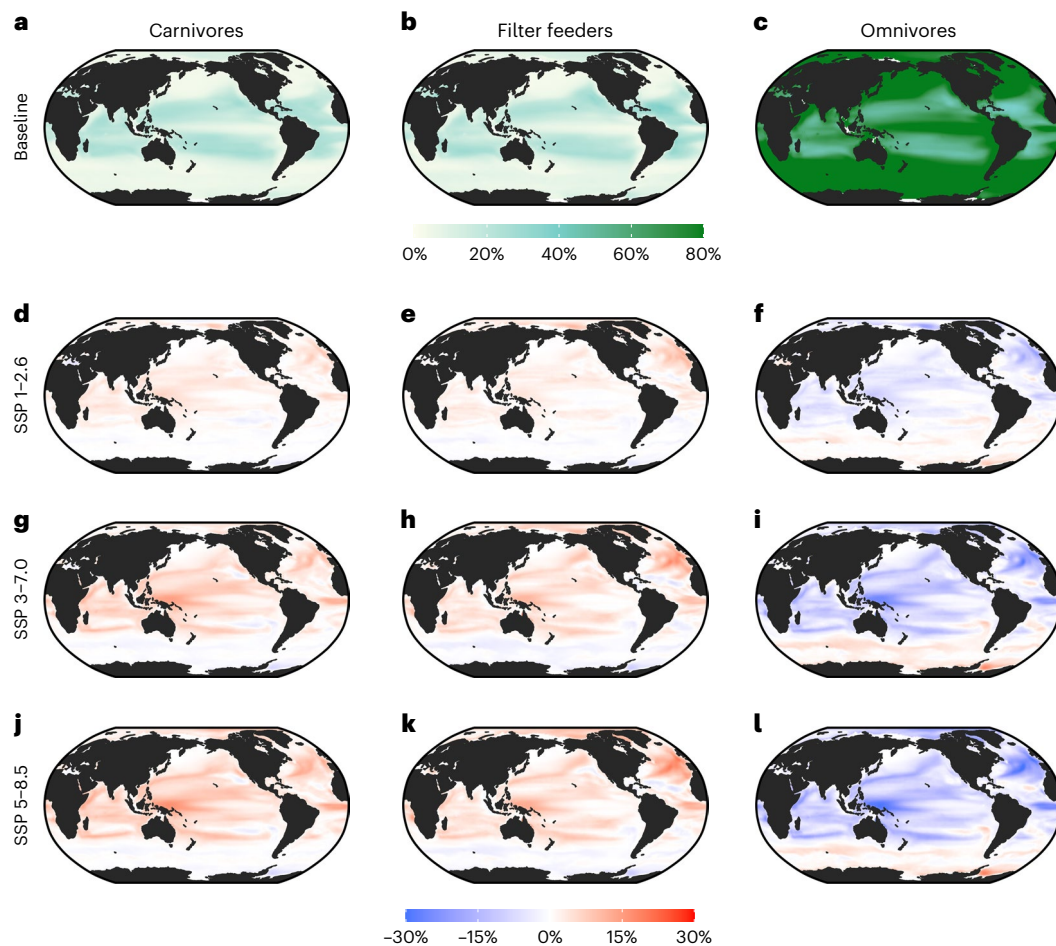


Fig. 3 | Climate-induced shifts in zooplankton community composition. a–c, The mean baseline percentage of total community biomass in 1980–2000 comprising carnivores (a), filter feeders (b) and omnivores (c). d–l, Maps of the mean change (%) of total zooplankton community biomass from carnivores

(d,g,j), filter feeders (e,h,k) and omnivores (f,i,l) in 2080–2100 relative to 1980–2000 under emission scenarios SSP 1–2.6 (d–f), SSP 3–7.0 (g–i) and SSP 5–8.5 (j–l), across the five Earth-system models used to force ZooMSS.

Since warming affects all zooplankton groups in ZooMSS in the same way (section on The model), projected shifts are driven primarily by changes in phytoplankton size structure. Under climate change, picophytoplankton are projected to increase as a proportion of the phytoplankton community across most of the world's oceans^{33,34}, with corresponding declines in the prevalence of larger phytoplankton (Extended Data Fig. 4d–l). Owing to their massive PPMRs (Supplementary Table 1), filter feeders consume picophytoplankton^{25,35} (Extended Data Fig. 2e,g), which are too small for most copepods and euphausiids. Thus, filter-feeding zooplankton can outcompete omnivores in oligotrophic regions^{8,14,24}. Carnivores are also projected to increase as a proportion of the zooplankton community because of the greater relative importance of microzooplankton^{8,14,36} (Supplementary Fig. 4), which is >50% of their diet (Extended Data Fig. 2m,o). Finally, the greater prevalence of picophytoplankton (Extended Data Fig. 4, left column) and microzooplankton (Supplementary Fig. 4) and projected declines in larger phytoplankton in the future (Extended Data Fig. 4, centre and right column), decreases the total phytoplankton directly available for omnivorous zooplankton^{8,14,36}, since nanophytoplankton and microphytoplankton are large components of their diet, especially in eutrophic waters (Extended Data Fig. 2i,k).

Within carnivore and filter-feeder groups, jellyfish (Supplementary Fig. 1, right column) and larvaceans (Supplementary Fig. 2, left column) experienced modest declines in some parts of the open-ocean gyres, whereas the other filter feeders (salps) and

carnivores (carnivorous copepods and chaetognaths) increased as a proportion of total zooplankton biomass. These unique changes for larvaceans and jellyfish are driven not only by shifts in phytoplankton community size structure but also predator–prey interactions among zooplankton groups. For example, larvaceans are the smallest mesozooplankton (Supplementary Table 1) and their declines in some regions where salps increase as a proportion of the zooplankton are probably driven by increases in predation pressure not balanced by growth, as they become more prevalent in diets of carnivores and SPF as oligotrophic regions expand (Extended Data Fig. 2m,o,q,s). Conversely for jellyfish, their declines in some regions where other carnivores increase are driven by decreases in the prevalence of omnivorous copepods (Supplementary Fig. 3, left column) and larvaceans (Supplementary Fig. 2, left column), which together are >50% of jellyfish diet from oligotrophic to eutrophic waters (Extended Data Fig. 2q).

Evidence for this projected shift from omnivores toward carnivores and gelatinous filter feeders has already been observed in some regions^{37,38} and our results suggest that these shifts will intensify under climate change. Only in the Southern Ocean and some subtropical waters where larger microphytoplankton increase as a proportion of the phytoplankton community (Extended Data Fig. 4, right column) is the dominance of omnivorous zooplankton projected to increase (Fig. 3f,i,l). However, effects of climate change on phytoplankton in the Southern Ocean are poorly understood³⁹, which means our

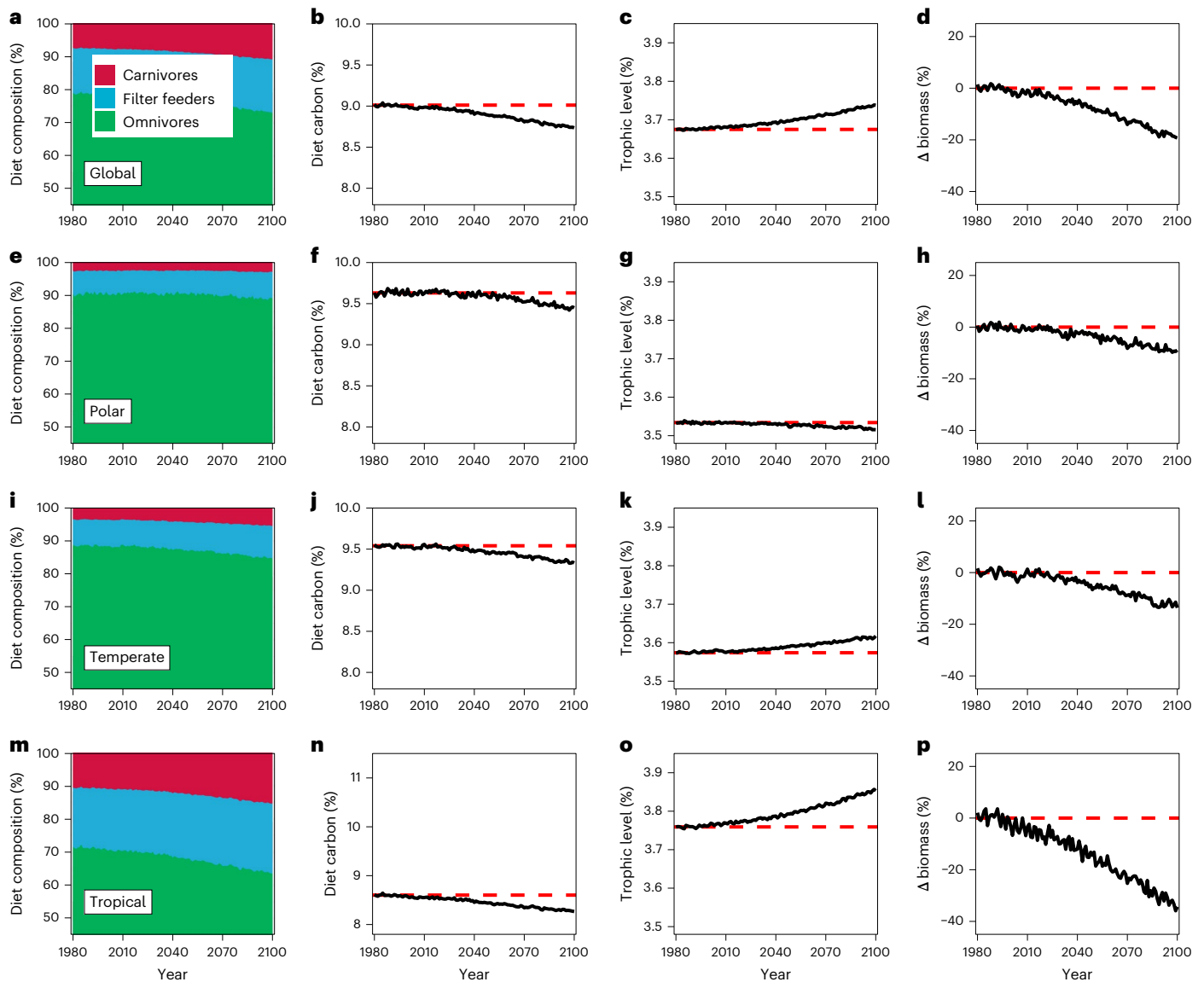


Fig. 4 | Effects of climate change on SPF. **a–p**, Mean change in the diet composition (**a,e,i,m**), diet carbon (**b,f,j,n**), trophic level (**c,g,k,o**) and biomass (**d,h,i,p**) of SPF, relative to 1980–2000 under SSP 5–8.5 in global (**a–d**), polar

(**e–h**), temperate (**i–l**) and tropical (**m–p**) waters, across the five Earth-system models used to force ZooMSS in this study. Extended Data Figure 10 gives a map of the biomes. Dashed red lines represent the mean in 1980–2000.

projections of zooplankton community shifts in this region are particularly uncertain. Nevertheless, these results represent substantial potential shifts in global zooplankton composition, given that omnivorous copepods dominate total zooplankton biomass³⁴ and are arguably the most abundant multicellular animals on Earth³⁵.

Implications for fish

Changes in zooplankton composition can have profound implications for fish^{1,13,16,29,36,40}. We thus explored how changes in zooplankton community composition under SSP 5–8.5 affected the diet and trophic level of SPF. SPF have an extremely important ecological role transferring energy to larger fish and form some of the most economically valuable fisheries resources, contributing significantly to global food security⁴¹.

Globally, the proportion of SPF diet comprising omnivorous zooplankton decreased from 79 to 72% between 1980 and 2100, with simultaneous increases in the contribution of filter feeders from 13 to 16% and carnivores from 8 to 12% (Fig. 4a). These changes in SPF diet mirrored shifts in zooplankton community composition (Extended Data Fig. 5a). Yet, despite future declines in omnivorous zooplankton

(high PPMRs) and increases in carnivorous zooplankton (low PPMRs) that should lead to longer food chains^{8,42,43}, the mean trophic level of SPF increased by only -1.5% globally (from 3.67 to 3.74) and by at most -2.5% in tropical waters (from 3.76 to 3.86) from 1980 to 2100 (Fig. 4, third column). In contrast, the mean trophic level of omnivorous zooplankton increased by on average 3.5% (from 2.57 to 2.66) in tropical waters and 2.5% (from 2.46 to 2.52) globally (Extended Data Fig. 6, right column). These mean changes conceal greater increases within regions. For example, the trophic level of omnivorous zooplankton increased by $\geq 15\%$ in some areas in the North Atlantic but $\leq 8\%$ for SPF in the same areas (Extended Data Fig. 7c,d). The smaller changes in SPF trophic level are because the longer food chains resulting from a rise in carnivores and decline in omnivores are partially offset by the increase in gelatinous filter feeders in the diet of SPF (Fig. 4, first column). Owing to their huge PPMRs and similar body size range to omnivores (Supplementary Table 1), filter feeders are uniquely capable of shunting energy from small phytoplankton to higher trophic levels^{32,35,44}. These traits mean that the trophic level of filter feeders in ZooMSS in the future falls within a

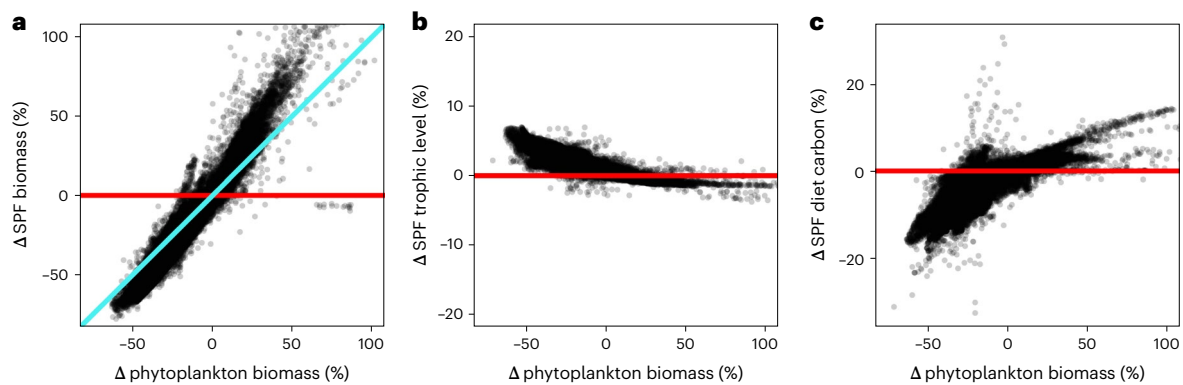


Fig. 5 | Effects of changing phytoplankton biomass on SPF. a–c. Mean percentage change in the biomass (a), trophic level (b) and diet carbon content (c) of SPF against the percentage change in phytoplankton biomass, for individual 1° grid squares from 1980–2000 to 2080–2100 under the SSP 5–8.5 emissions scenario across the five Earth-system models used to force ZooMSS in this study. Under the blue 1–1 line in a, where the change in phytoplankton

biomass is negative is where the decline in SPF biomass is greater than that of phytoplankton. Similarly, above the blue 1–1 line in a and where the change in phytoplankton biomass is positive, is where the increase in SPF biomass is greater than that of phytoplankton. The red solid horizontal line in each figure indicates where the percentage change in each SPF attribute is zero.

relatively constant and low range of 2–2.25, while trophic levels of omnivores are more sensitive to shifts in phytoplankton biomass from oligotrophic to eutrophic waters compared to filter feeders (Extended Data Fig. 2 and Extended Data Fig. 6, centre and right column; Extended Data Fig. 7). Our results suggest that the trophic stability of filter feeders will moderate effects of shrinking phytoplankton on future trophic levels of SPF. At the same time, carnivorous jellyfish have large PPMRs relative to other carnivores (Supplementary Table 1), although their large body sizes mean they are more a competitor of SPF than prey (Extended Data Fig. 2q–t). Thus, the role of jellyfish in buffering the effects of climate change on food web length could be minor compared to filter feeders.

The unique role of gelatinous filter feeders in providing an alternative energy pathway between phytoplankton and higher trophic levels has long been suggested^{35,44}. However, owing to their fragile bodies, gelatinous zooplankton have been poorly studied because they rapidly disintegrate in the guts of predators or when sampled in nets²⁴. New approaches to examining diets of marine predators, such as stable isotope analysis and DNA metabarcoding, show that gelatinous filter feeders are often important prey of many commercial fish species and therefore serve an important role in structuring marine ecosystems^{27–29,32}. Our results suggest that the direct energy pathway from small phytoplankton through filter feeders to fish will grow in importance if small phytoplankton become increasingly dominant under climate change³³.

The trend toward gelatinous zooplankton caused a decrease in the carbon content of SPF diets under climate change (Fig. 4, second column). Gelatinous carnivores such as jellyfish and chaetognaths and filter feeders such as larvaceans and salps, are 65–95% less carbon-dense than omnivorous zooplankton such as euphausiids and copepods¹⁷. As gelatinous zooplankton outcompete carbon-dense omnivorous groups, the carbon content of the diet of SPF decreased by -3.5% globally, from just over 9% in 1980 to 8.7% in 2100 (Fig. 4b). Although this mean global decline is modest, there was a greater mean reduction of -4.5% in the tropical biome (1980–2100; Fig. 4n). These shifts in the nutritional quality of SPF diets reflect changes in zooplankton community carbon content in these biomes (Extended Data Fig. 5, right column).

Sudden, climate-driven changes in fish diets have already been observed during the recent marine heatwave in the North Pacific from 2013 to 2016, commonly called the ‘Blob’, which led to hotter sea-surface temperatures and lower primary production⁴⁵. Decreases in phytoplankton production during the heatwave drove declines in the

abundance of carbon-dense euphausiids and increases in carbon-poor gelatinous zooplankton⁴⁶, which then manifested as shifts in the diet of SPF⁴⁷ as well as declines in their weight and energetic content^{47,48}. Coupled with these empirical studies, our results indicate future fish communities in large parts of the world’s oceans face not only reduced carrying capacity from falling primary production but also potentially lower carbon diets as reductions in phytoplankton biomass favour less carbon-dense zooplankton communities (Extended Data Fig. 8).

From 1980 to 2100, global SPF biomass is projected to decline by 20% (from 1980 to 2100) under SSP 5–8.5, with declines of -10–35% within biomes (Fig. 4, fourth column). Similar declines are also projected for total fish biomass (Supplementary Fig. 5). Declines in SPF biomass were slightly greater than phytoplankton in many regions (Fig. 5a), a process known as trophic amplification²². To assess whether an increasingly gelatinous zooplankton community played a role in trophic amplification from phytoplankton to fish, we ran ZooMSS with the carbon content of all zooplankton groups held constant at 10%, the same as SPF (Supplementary Table 1). The magnitude of declines in SPF biomass in tropical waters were about 10% smaller (~32% versus ~35%) when zooplankton carbon contents were held constant (Extended Data Fig. 9). At the same time, in temperate waters where there was little change in zooplankton composition, there was almost no difference in the change in SPF biomass (Extended Data Fig. 9c) and in polar waters, declines in fish biomass were slightly larger (Extended Data Fig. 9b) when zooplankton carbon contents were held constant.

Discussion

A general expectation of climate change is that future marine ecosystems will support less fish biomass where primary production decreases^{5,30,49,50}, while the number of trophic steps between primary producers and fish is expected to substantially increase as mean phytoplankton size declines^{42,43}. Our results support the first part of this expectation—less phytoplankton means lower fish biomass (Fig. 5a)—while challenging the expectation that future food webs will be much longer (Figs. 4, third column and 5b). Our results also support another suggestion: lower future phytoplankton biomass will support more gelatinous food webs (Fig. 5c and Extended Data Fig. 8).

In ZooMSS, shifts in phytoplankton size structure are the primary driver of zooplankton composition shifts. However, empirical evidence^{18,51} and a recent modelling study⁵² suggest that gelatinous filter feeders and carnivore (including jellyfish) biomass may increase because of temperature alone, which is not resolved in ZooMSS. This means that ZooMSS could still underestimate the role of gelatinous

zooplankton in structuring marine food webs in future, warmer oceans. At the same time, ZooMSS may also underestimate the buffering capacity of gelatinous filter feeders on fish biomass under climate change^{33,34} because it does not resolve how gelatinous filter feeders are more easily caught²⁷ and digested²⁴ by fish compared to more carbon-dense copepods and euphausiids. Finally, direct human impacts from fishing—also not considered here—have also been suggested to favour carnivorous jellyfish by removing their predators and competitors⁵³, although this idea remains disputed⁵⁴.

Since ZooMSS was designed to project the condition of marine ecosystems over large spatial and temporal scales, it has many simplifying assumptions concerning dynamic processes such as reproduction, seasonality and adaptation (section on Model caveats). This means that we are likely to be underestimating climate effects on marine ecosystems at finer spatial and temporal scales. For instance, decoupling between higher trophic level reproduction and seasonal phytoplankton pulses in polar and temperate regions under climate change could drive increasingly widespread recruitment failures, with cascading effects across marine food webs^{55,56}. By using an annual time step, these processes and their effects are not explicitly represented here. Further, as zooplankton and fish groups in ZooMSS are defined by fixed functional traits (Supplementary Table 1), any potential adaptations to changing environmental conditions are also not considered. More broadly, the coupling between phytoplankton and consumers in ZooMSS—and most of the current generation of marine ecosystem models—is incomplete, with models not resolving predation impacts from higher trophic levels on phytoplankton³⁰. This lack of coupling means that potential critical pathways of trophic amplification remain unresolved.

Nevertheless, we believe our model is an important step towards resolving the changing role of zooplankton under climate change. Previous studies have highlighted the sensitivity of global higher trophic level biomass to energy flow through the plankton^{16,22,57} but at present ZooMSS is the only global marine ecosystem model that resolves zooplankton by multiple functional traits³⁰. At the same time, although an increasing number of biogeochemical models now resolve gelatinous zooplankton and their role in carbon sequestration^{52,58,59}, they do not explicitly represent fish. By bridging the gap between plankton and fish, the trait-based modelling framework used here is a powerful way to generate new insights into how climate change will affect zooplankton and the pivotal role they play in the world's marine ecosystems.

Online content

Any methods, additional references, Nature Portfolio reporting summaries, source data, extended data, supplementary information, acknowledgements, peer review information; details of author contributions and competing interests; and statements of data and code availability are available at <https://doi.org/10.1038/s41558-023-01630-7>.

References

- Mitra, A. et al. Bridging the gap between marine biogeochemical and fisheries sciences; configuring the zooplankton link. *Prog. Oceanogr.* **129**, 176–199 (2014).
- Bucklin, A. et al. in *Life in the World's Oceans: Diversity, Distribution, and Abundance* (ed. McIntyre, A. D.) 247–265 (Wiley, 2010).
- Hatton, I. A., Heneghan, R. F., Bar-On, Y. M. & Galbraith, E. D. The global ocean size-spectrum from bacteria to whales. *Sci. Adv.* **7**, eabh3732 (2021).
- Everett, J. D. et al. Modeling what we sample and sampling what we model: challenges for zooplankton model assessment. *Front. Mar. Sci.* **4**, 77 (2017).
- Tittensor, D. P. et al. Next-generation ensemble projections reveal higher climate risks for marine ecosystems. *Nat. Clim. Change* **11**, 973–981 (2021).
- Bopp, L. et al. Multiple stressors of ocean ecosystems in the 21st century: projections with CMIP5 models. *Biogeosciences* **10**, 6225–6245 (2013).
- Litchman, E., Ohman, M. D. & Kiørboe, T. Trait-based approaches to zooplankton communities. *J. Plankton Res.* **35**, 473–484 (2013).
- Boyce, D. G., Frank, K. T. & Leggett, W. C. From mice to elephants: overturning the 'one size fits all' paradigm in marine plankton food chains. *Ecol. Lett.* **18**, 504–515 (2015).
- Benedetti, F. et al. Major restructuring of marine plankton assemblages under global warming. *Nat. Commun.* **12**, 5526 (2021).
- Steinberg, D. K. & Landry, M. R. Zooplankton and the ocean carbon cycle. *Ann. Rev. Mar. Sci.* **9**, 413–444 (2017).
- Boyd, P. W., Claustre, H., Levy, M., Siegel, D. A. & Weber, T. Multifaceted particle pumps drive carbon sequestration in the ocean. *Nature* **568**, 327–335 (2019).
- Böckmann, S. et al. Salp fecal pellets release more bioavailable iron to Southern Ocean phytoplankton than krill fecal pellets. *Curr. Biol.* **31**, 2737–2746 (2021).
- Dam, H. G. & Baumann, H. *Climate Change Impacts on Fisheries and Aquaculture: A Global Analysis* Vol. 1, Ch. 25 (John Wiley, 2017).
- Barton, A. D. et al. The biogeography of marine plankton traits. *Ecol. Lett.* **16**, 522–534 (2013).
- Hansen, B., Bjornsen, P. K. & Hansen, P. J. The size ratio between planktonic predators and their prey. *Limnol. Oceanogr.* **39**, 395–403 (1994).
- Heneghan, R. F., Everett, J. D., Blanchard, J. L. & Richardson, A. J. Zooplankton are not fish: improving zooplankton realism in size-spectrum models mediates energy transfer in food webs. *Front. Mar. Sci.* **3**, 201 (2016).
- McConville, K., Atkinson, A., Fileman, E. S., Spicer, J. I. & Hirst, A. G. Disentangling the counteracting effects of water content and carbon mass on zooplankton growth. *J. Plankton Res.* **39**, 246–256 (2017).
- Heneghan, R. F. et al. A functional size-spectrum model of the global marine ecosystem that resolves zooplankton composition. *Ecol. Model.* **435**, 109265 (2020).
- van Vuuren, D. P. et al. The Shared Socio-economic Pathways: trajectories for human development and global environmental change. *Glob. Environ. Change* **42**, 148–152 (2017).
- Eyring, V. et al. Overview of the Coupled Model Intercomparison Project Phase 6 (CMIP6) experimental design and organization. *Geosci. Model Dev.* **9**, 1937–1958 (2016).
- Kwiatkowski, L., Aumont, O. & Bopp, L. Consistent trophic amplification of marine biomass declines under climate change. *Glob. Change Biol.* **25**, 218–229 (2019).
- Stock, C. A., Dunne, J. P. & John, J. G. Drivers of trophic amplification of ocean productivity trends in a changing climate. *Biogeosciences* **11**, 7125–7135 (2014).
- Landry, M. R. & Calbet, A. Microzooplankton production in the oceans. *ICES J. Mar. Sci.* **61**, 501–507 (2004).
- Henschke, N., Everett, J. D., Richardson, A. J. & Suthers, I. M. Rethinking the role of salps in the ocean. *Trends Ecol. Evol.* **31**, 720–733 (2016).
- Wirtz, K. W. Who is eating whom? Morphology and feeding type determine the size relation between planktonic predators and their ideal prey. *Mar. Ecol. Prog. Ser.* **445**, 1–12 (2012).
- Llopiz, J. K., Richardson, D. E., Shiroza, A., Smith, S. L. & Cowen, R. K. Distinctions in the diets and distributions of larval tunas and the important role of appendicularians. *Limnol. Oceanogr.* **55**, 983–996 (2010).
- Cardona, L., de Quevedo, I. Á., Borrell, A. & Aguilar, A. Massive consumption of gelatinous plankton by Mediterranean apex predators. *PLoS ONE* **7**, e31329 (2012).

28. Hays, G. C., Doyle, T. K. & Houghton, J. D. R. A paradigm shift in the trophic importance of jellyfish? *Trends Ecol. Evol.* **33**, 874–884 (2018).
29. Richardson, A. J. & Schoeman, D. S. Climate impact on plankton ecosystems in the Northeast Atlantic. *Science* **305**, 1609–1612 (2004).
30. Heneghan, R. F. et al. Disentangling diverse responses to climate change amongst global marine ecosystem models. *Prog. Oceanogr.* **198**, 102659 (2021).
31. McGinty, N., Barton, A. D., Record, N. R., Finkel, Z. V. & Irwin, A. J. Traits structure copepod niches in the North Atlantic and Southern Ocean. *Mar. Ecol. Prog. Ser.* **601**, 109–126 (2018).
32. Jaspers, C., Nielsen, T. G., Carstensen, J., Hopcroft, R. R. & Møller, E. F. Metazooplankton distribution across the Southern Indian Ocean with emphasis on the role of Larvaceans. *J. Plankton Res.* **31**, 525–540 (2009).
33. Morán, X. A. G., López-Urrutia, Á., Calvo-Díaz, A. & Li, W. K. W. Increasing importance of small phytoplankton in a warmer ocean. *Glob. Change Biol.* **16**, 1137–1144 (2010).
34. Henson, S. A., Cael, B. B., Allen, S. R. & Dutkiewicz, S. Future phytoplankton diversity in a changing climate. *Nat. Commun.* **12**, 5372 (2021).
35. Conley, K. R., Lombard, F. & Sutherland, K. R. Mammoth grazers on the ocean's minuteness: a review of selective feeding using mucous meshes. *Proc. R. Soc. B* **285**, 20180056 (2018).
36. Jennings, S. & Warr, K. J. Smaller predator–prey body size ratios in longer food chains. *Proc. R. Soc. B* **270**, 1413–1417 (2003).
37. Atkinson, A., Siegel, V., Pakhomov, E. & Rothery, P. Long-term decline in krill stock and increase in salps within the Southern Ocean. *Nature* **432**, 100–103 (2004).
38. Schmidt, K. et al. Increasing picocyanobacteria success in shelf waters contributes to long-term food web degradation. *Glob. Change Biol.* **26**, 5574–5587 (2020).
39. Deppeler, S. L. & Davidson, A. T. Southern Ocean phytoplankton in a changing climate. *Front. Mar. Sci.* **4**, 40 (2017).
40. Richon, C. & Tagliabue, A. Biogeochemical feedbacks associated with the response of micronutrient recycling by zooplankton to climate change. *Glob. Change Biol.* **27**, 4758–4770 (2021).
41. Peck, M. A. et al. Small pelagic fish in the new millennium: a bottom-up view of global research effort. *Prog. Oceanogr.* **191**, 102494 (2021).
42. Ryther, J. H. Photosynthesis and fish production in the sea. *Science* **166**, 72–76 (1969).
43. Eddy, T. D. et al. Energy flow through marine ecosystems: confronting transfer efficiency. *Trends Ecol. Evol.* **36**, 76–86 (2021).
44. Diebel, D. & Lee, S. H. Retention efficiency of submicron particles by the pharyngeal filter of the pelagic tunicate *Ioopleura vanhoeffeni*. *Mar. Ecol. Prog. Ser.* **81**, 25–30 (1992).
45. Yang, B., Emerson, S. R. & Angelica Penã, M. The effect of the 2013–2016 high temperature anomaly in the subarctic Northeast Pacific (the 'blob') on net community production. *Biogeosciences* **15**, 6747–6759 (2018).
46. Brodeur, R. D., Auth, T. D. & Phillips, A. J. Major shifts in pelagic micronekton and macrozooplankton community structure in an upwelling ecosystem related to an unprecedented marine heatwave. *Front. Mar. Sci.* **6**, 212 (2019).
47. Brodeur, R. D., Hunsicker, M. E., Hann, A. & Miller, T. W. Effects of warming ocean conditions on feeding ecology of small pelagic fishes in a coastal upwelling ecosystem: a shift to gelatinous food sources. *Mar. Ecol. Prog. Ser.* **617–618**, 149–163 (2019).
48. Piatt, J. F. et al. Extreme mortality and reproductive failure of common murrelets resulting from the northeast Pacific marine heatwave of 2014–2016. *PLoS ONE* **15**, e0226087 (2020).
49. Worm, B. et al. Rebuilding global fisheries. *Science* **325**, 578–585 (2009).
50. Lotze, H. K. et al. Ensemble projections of global ocean animal biomass with climate change. *Proc. Natl Acad. Sci. USA* **116**, 12907–12912 (2019).
51. Bouquet, J.-M. et al. Increased fitness of a key appendicularian zooplankton species under warmer, acidified seawater conditions. *PLoS ONE* **13**, e0190625 (2018).
52. Wright, R. M., Le Quéré, C., Buitenhuis, E., Pitois, S. & Gibbons, M. J. Role of jellyfish in the plankton ecosystem revealed using a global ocean biogeochemical model. *Biogeosciences* **18**, 1291–1320 (2021).
53. Richardson, A. J., Bakun, A., Hays, G. C. & Gibbons, M. J. The jellyfish joyride: causes, consequences and management responses to a more gelatinous future. *Trends Ecol. Evol.* **24**, 312–322 (2009).
54. Condon, R. H. et al. Recurrent jellyfish blooms are a consequence of global oscillations. *Proc. Natl Acad. Sci. USA* **110**, 1000–1005 (2013).
55. Edwards, M. & Richardson, A. J. Impact of climate change on marine pelagic phenology and trophic mismatch. *Nature* **430**, 881–884 (2004).
56. Durant, J. M. et al. Contrasting effects of rising temperatures on trophic interactions in marine ecosystems. *Sci. Rep.* **9**, 15213 (2019).
57. Jennings, S. & Collingridge, K. Predicting consumer biomass, size-structure, production, catch potential, responses to fishing and associated uncertainties in the world's marine ecosystems. *PLoS ONE* **10**, e0133794 (2015).
58. Luo, J. Y., Stock, C. A., Henschke, N., Dunne, J. P. & O'Brien, T. D. Global ecological and biogeochemical impacts of pelagic tunicates. *Prog. Oceanogr.* **205**, 102822 (2022).
59. Clerc, C., Aumont, O. & Bopp, L. *Current and Future Contribution of Filter-feeding Gelatinous Zooplankton to Global Marine Biogeochemistry* (EGU General Assembly, 2022); <https://doi.org/10.5194/egusphere-egu22-8584>

Publisher's note Springer Nature remains neutral with regard to jurisdictional claims in published maps and institutional affiliations.

Open Access This article is licensed under a Creative Commons Attribution 4.0 International License, which permits use, sharing, adaptation, distribution and reproduction in any medium or format, as long as you give appropriate credit to the original author(s) and the source, provide a link to the Creative Commons license, and indicate if changes were made. The images or other third party material in this article are included in the article's Creative Commons license, unless indicated otherwise in a credit line to the material. If material is not included in the article's Creative Commons license and your intended use is not permitted by statutory regulation or exceeds the permitted use, you will need to obtain permission directly from the copyright holder. To view a copy of this license, visit <http://creativecommons.org/licenses/by/4.0/>.

© The Author(s) 2023

Methods

The model

We use the ZooMSS (v.2.1)¹⁸, which uses the functional size-spectrum framework⁶⁰ to resolve multiple zooplankton and fish groups. In brief, ZooMSS resolves a single phytoplankton community, nine of the most prevalent zooplankton functional groups (heterotrophic flagellates and ciliates, omnivorous and carnivorous copepods, larvaceans, salps, euphausiids, chaetognaths and jellyfish) and three fish groups. The nine zooplankton groups are defined by their size ranges, feeding characteristics (PPMR and feeding kernel width) and carbon content. The three size-based fish groups are defined by their size ranges, broadly representing: small pelagic (planktivorous) fish ≤ 100 g, medium pelagic fish $100 \text{ g} \leq 10 \text{ kg}$ and large pelagic fish $10 \text{ kg} \leq 1 \text{ t}$. Other than their asymptotic size, the three fish groups share the same functional traits (feeding characteristics and carbon content), which are unique from the zooplankton groups. A summary of the parameter values used to define the functional traits of the nine zooplankton and three fish communities can be found in Supplementary Table 1. The version of ZooMSS used here has been slightly updated from the previous iteration (v.2.0)¹⁸. Carbon contents of flagellates, copepods, larvaceans and salps have been updated to better reflect published estimates, and the size range of flagellates has been expanded to incorporate nanoflagellates ($< 3 \mu\text{m}$). These updates result in very minor changes to model outputs compared to the previous iteration. To aid interpretation, in the main text we aggregated the output from the seven mesozooplankton and macrozooplankton types into three summary groups on the basis of their feeding characteristics: omnivores (omnivorous copepods and euphausiids), carnivores (carnivorous copepods, chaetognaths and jellyfish) and filter feeders (larvaceans and salps). Heterotrophic flagellates and ciliates were grouped together as microzooplankton.

Zooplankton and fish growth at any size class is driven by the density of smaller organisms within their preferred prey size range. For predators, growth conversion efficiency—the proportion of consumed food converted into new wet weight biomass—is affected by the carbon content of their prey. Prey groups with larger carbon contents (for example, copepods) contribute more to the growth of their predators when they are consumed than other groups with less carbon (for example, jellyfish). From the perspective of the prey, total predation from larger size classes is the primary source of mortality. Since individuals grow and age over time, senescence mortality is also included, which increases with body size.

ZooMSS is driven by sea-surface temperature and phytoplankton variables (see next section on Environmental drivers). Across the global ocean, zooplankton community composition emerges based on the relative fitness of the different groups. Since temperature affects all groups in the same way, it is a secondary driver of total zooplankton biomass (since background mortality from senescence increases with temperature) and not a major driver of zooplankton composition. Rather, zooplankton composition is primarily driven by shifts in the size structure of the phytoplankton, from oligotrophic to eutrophic waters (Supplementary Fig. 14).

Spatial patterns of zooplankton groups generally agree with observations, as do growth rates of the functional groups¹⁸. However, the zooplankton abundance modelled in ZooMSS is considerably higher than observations¹⁸. This could be due to the abundance estimates of zooplankton in ZooMSS including all size classes—eggs, nauplii, larvae, juveniles and adults—whereas observations from nets severely underestimate early life stages and thus abundances⁴. At the same time, total zooplankton biomass from ZooMSS across the global ocean is within the range of two empirical estimates^{18,61}. However, this does not mean that ZooMSS could not be within the range of empirical estimates for the wrong reasons or due to compensation effects.

Environmental drivers

ZooMSS is run with sea-surface temperature and phytoplankton variables averaged annually, with a 1° spatial resolution. With respect

to phytoplankton variables, at minimum ZooMSS requires surface chlorophyll *a* from Earth-system models or satellite to calculate the size structure of the phytoplankton community. However, where available, mean size-fractionated phytoplankton biomass across the euphotic zone can also be used to calculate continuous phytoplankton size spectra.

Temperature affects the growth and mortality rates of the zooplankton and fish functional groups. Temperature is incorporated into growth and mortality rates with a Q_{10} factor of 2, meaning that for every 10°C of warming, all growth and mortality rates of zooplankton and fish are accelerated twofold. We chose a Q_{10} factor of 2 based on the comprehensive review of zooplankton growth rates⁶², which contained $> 2,500$ observations across nine zooplankton taxonomic groups (non-copepod crustaceans, copepods, cnidarians, ctenophores, chaetognaths, pteropods, polychaetes, thaliaceans and larvaceans). They found Q_{10} values ranged from 0.38 to 3.86, with a median of 1.86, although when individual body size was accounted for the median Q_{10} value shifted to 2.31. We selected a Q_{10} factor of 2 for zooplankton and fish since it falls between these two median estimates and is also almost identical to the body-size adjusted Q_{10} value of 1.98 for teleost fish⁶³.

Chlorophyll *a* sets the total biomass and size structure of the phytoplankton community, since phytoplankton dynamics are not explicitly represented in ZooMSS. Phytoplankton community slope, intercept and maximum size is calculated in several steps. First, we use the algorithm from ref. ⁶⁴, which estimates the percentage contribution of picophytoplankton (0.2–2 μm equivalent spherical diameter (ESD)), nanophytoplankton (2–20 μm ESD) and microphytoplankton ($> 20 \mu\text{m}$ ESD) to total chlorophyll *a* in surface waters. This algorithm describes changes in the phytoplankton community composition across the ocean: picophytoplankton dominate in oligotrophic waters but decline as a percentage of the community as chlorophyll *a* concentration increases; nanophytoplankton are most prevalent in mesotrophic waters; and microphytoplankton are a minor component at low chlorophyll concentration but increase from oligotrophic to eutrophic waters (Supplementary Fig. 12). Second, as the chlorophyll:carbon ratio of phytoplankton varies across the oceans of the world⁶⁵, the contribution of each of the three phytoplankton groups to total chlorophyll *a* is then converted to carbon biomass using the empirical relationship from Fig. 1c of ref. ⁶⁵. Phytoplankton carbon biomass is converted to wet weight assuming 1 g carbon weight = 10 g wet weight⁶⁶. Last, for each 1° grid cell and each year, phytoplankton community slope, intercept and maximum size are then found analytically using the wet weight biomass of the three phytoplankton groups (see the supplement of ref. ¹⁸ for more information). Derived phytoplankton abundance slopes range from -1.2 to -0.77 from waters low to high in chlorophyll *a*, which is similar to ranges reported in empirical studies^{67–69}.

When size-fractionated phytoplankton carbon biomass variables are available from Earth-system models, the conversion step from chlorophyll *a* to carbon described above is not required, nor the size-fractionation step involving the Brewin algorithm⁷⁰. Using size-fractionated phytoplankton directly from Earth-system models also means that subsurface features of the phytoplankton—such as the deep chlorophyll maximum in stratified waters⁷¹—are incorporated in continuous phytoplankton size spectra for stratified waters (provided these features are present in the Earth-system model phytoplankton).

Of the five Earth-system models used in this study, size-fractionated and depth-resolved phytoplankton carbon biomass was available from CESM2 and GFDL-ESM4. However, we were only able to use these products from GFDL-ESM4 but not CESM2. This was because there is an inconsistency between overall phytoplankton biomass of CESM2 and the size structure of its phytoplankton community. It is well-established empirically that as total phytoplankton biomass increases, the proportion of the phytoplankton that comes from large size classes increases^{8,64,72–74}. In CESM2, this relationship exists but it is relatively weak. For example, for most of the global ocean where

mean phytoplankton biomass in the euphotic zone is between 0.05 and 0.15 g m⁻³ the proportion of phytoplankton from large size classes can vary between -10% and 90% in CESM2, before sharply increasing to >90% for waters with phytoplankton >0.15 g m⁻³. In contrast, the change in the proportion of phytoplankton from large size classes in GFDL-ESM4 increases smoothly from -2% to 70%, across waters with low to high phytoplankton biomass (Supplementary Fig. 13a). As a result, we found it was not possible to consistently convert small and large phytoplankton biomass from CESM2 to continuous phytoplankton size spectra; total phytoplankton biomass from CESM2-derived continuous size spectra does not match what is provided from the ESM itself, a challenge that is not present with GFDL-ESM4-derived phytoplankton spectra (Supplementary Fig. 13b). Therefore, for GFDL-ESM4, we used size-fractionated and depth-resolved phytoplankton carbon biomass to calculate continuous phytoplankton size spectra but, for CESM2 and the other Earth-system models, we used surface chlorophyll *a* concentration.

To assess how using either surface chlorophyll *a* or size-fractionated phytoplankton could alter our results, we compared changes in the ZooMSS zooplankton community composition for GFDL-ESM4 simulations that have both phytoplankton outputs available under SSP 5–8.5. Spatial patterns of contemporary phytoplankton size structure and zooplankton composition, as well as future changes in both were broadly similar between the two approaches with GFDL-ESM4 (Supplementary Figs. 6–9). However, in polar and tropical biomes, mean climate-driven increases in picophytoplankton as a proportion of the total phytoplankton were lower (-0% versus 2% in polar waters and -6% versus 8% in tropical waters) when depth-resolved phytoplankton was used compared to surface chlorophyll *a* (Supplementary Fig. 10). This smaller change slightly reduced the increase in the proportion of the total zooplankton from filter feeders (-0% versus 2% in polar waters and -6% versus 8% in tropical waters) and corresponding decrease in omnivores in these regions (Supplementary Fig. 11). All else being equal, this suggests that increases in the prevalence of gelatinous filter feeders at the expense of omnivores could be attenuated, depending on how phytoplankton community size structure is parameterized. However, uncertainty in projected shifts in plankton composition introduced when alternative inputs are used to calculate the continuous phytoplankton size-spectrum is much smaller than the total uncertainty across the five Earth-system models (Supplementary Figs. 10 and 11).

Model caveats

There are several caveats associated with ZooMSS. First, since ZooMSS is designed to provide insight into the long-term conditions of marine ecosystems over large spatial scales, we have made many simplifying assumptions about dynamic processes such as reproduction, seasonality and predator–prey coupling in the plankton. Zooplankton reproduction is a complex and diverse process, with groups exhibiting a variety of strategies such as binary fission in ciliates⁷⁵ and flagellates⁷⁶, alternating generations of sexual and asexual reproduction in salps⁷⁷ and jellyfish⁷⁸, hermaphroditism in chaetognaths⁷⁹ and intersexuality in copepods⁸⁰. What is more, since many zooplankton groups time their reproduction to coincide with phytoplankton blooms^{81,82} seasonal cycles of boom and bust in the phytoplankton is a major driver of variation of zooplankton productivity, particularly in polar and temperate areas. However, for simplicity, ZooMSS assumes constant recruitment for fish and zooplankton groups, as in some other size-spectrum models^{57,83}, which keeps the abundances of their smallest size classes fixed, relative to the abundance of other groups in the same size class. By simplifying reproduction and using a yearly temporal resolution for our model inputs, we do not explicitly resolve these reproductive and seasonal processes.

Second, another simplifying assumption in ZooMSS and other global marine ecosystem models is that the phytoplankton community is represented as a static resource because it is driven by external inputs (for example, satellite remote sensing or Earth-system models)

and thus has no predation feedback from higher trophic levels³⁰. However, at large temporal and spatial scales, the absence of an explicit two-way coupling between phytoplankton and zooplankton in ZooMSS does not lead to unrealistic estimates of zooplankton biomass or growth, since the model can reproduce global zooplankton biomass and growth rates within the range of empirical estimates¹⁸. Further, global zooplankton biomass declines under climate change are similar in ZooMSS to the range of projections from biogeochemical models that explicitly resolve predator–prey interactions between phytoplankton and zooplankton²¹. Yet, the absence of diverse zooplankton reproductive strategies and phytoplankton dynamics, from predation impacts to seasonal booms and busts, means that the current version of ZooMSS is not suitable for providing insight beyond long-term conditions of marine ecosystems over large spatial scales.

Third, the size structure estimated from the near-surface chlorophyll *a* is assumed to be representative of the phytoplankton community size structure more generally. Using near-surface chlorophyll *a* from four of the five Earth-system models used in this study means that ZooMSS does not resolve phytoplankton communities at the deep chlorophyll maximum layers, which are ubiquitous in low chlorophyll *a*, stratified regions⁷¹ and thus probably underestimates primary producer biomass in oligotrophic regions.

Fourth, and related to the second caveat, where size-fractionated, depth-resolved phytoplankton biomass is not available directly from the Earth-system models, ZooMSS does not resolve phytoplankton size structure through the upper water column. In these instances, we use surface chlorophyll *a* to represent the phytoplankton (where size-fractionated phytoplankton is not available from Earth-system models) because it is a key variable used by algorithms that calculate the global contribution of pico-, nano- and microphytoplankton to total phytoplankton biomass⁸⁴. This includes the algorithm used by ZooMSS, developed by ref. ⁶⁴, which we selected because it was calibrated using an extensive dataset of 5,841 in situ samples across all basins except the Arctic Ocean. To our knowledge, the algorithm of ref. ⁷⁴ is the only global algorithm that uses surface chlorophyll *a* to calculate phytoplankton community composition across the entire euphotic zone. However, ref. ⁷⁴ found that in stratified waters where the deep chlorophyll maximum is a persistent feature, the variation in phytoplankton size structure over 1.5 times the euphotic zone depth from oligotrophic to eutrophic waters was broadly similar to the variation in surface waters (comparing Fig. 6a and c in ref. ⁷⁴). Uncertainties remain around how phytoplankton size structure varies with depth at the global scale⁷⁴, as well as how phytoplankton at the individual and community level will respond to climate change^{64,85,86}. However, it is widely expected that the global dominance of small phytoplankton will increase^{34,86,87} as warm, nutrient-poor oligotrophic regions expand⁸⁸ and this expectation is the primary driver of the projected climate-driven changes in zooplankton composition in ZooMSS.

Although temperature sensitivity varies among taxa⁸⁹, ZooMSS uses a uniform Q_{10} across groups, as is common in many marine ecosystem and Earth-system models^{30,34,90–94}. This is because—to the best of our knowledge—a meta-analysis of the temperature dependence of physiological processes related to growth and mortality across broad zooplankton taxonomic groups does not yet exist. Since we use the same Q_{10} across all functional groups, temperature shifts have little effect on the relative competitiveness of different zooplankton groups in ZooMSS. Rather, all else being equal, increasing temperatures will primarily cause declines in biomass for all groups, due to increasing non-predation mortality (for example, senescence) that is not balanced by increases in predation-driven growth.

Finally, ZooMSS is not a hydrodynamic model and thus does not resolve passive (for example, by currents) or active movement of fish or zooplankton. This is a common weakness among other global marine ecosystem models^{91–94}. This could bias abundances in certain regions

due to active movement and migration of apex predators by swimming and by passive transport of zooplankton. Further, the lack of hydrodynamics means that ZooMSS does not include vertical mixing, which could affect zooplankton abundances, although the phytoplankton fields from Earth-system models used to drive ZooMSS do include hydrodynamic processes.

Running the model

Abundances of the zooplankton and fish groups were each governed by separate, second-order McKendrick–von Foerster equations, which we solved numerically using a second-order semi-implicit upwind finite difference scheme⁹⁵. For each 1° cell and for each year, ZooMSS is initialized with the same zooplankton composition¹⁸ and community structure then emerges, on the basis of the relative fitness of the different groups given environmental conditions. Previous sensitivity analysis has shown that total zooplankton biomass from the model is robust to ±50% changes in the initial abundance of each zooplankton group¹⁸.

For each simulation forced with temperature, chlorophyll *a* concentration or size-fractionated and depth-resolved phytoplankton biomass, we run the model for 1,000 years, with a half-weekly time step and the zooplankton and fish community size ranges discretized into 0.1 log₁₀ size intervals. The first 500 years is a burn-in period, allowing the different zooplankton groups to interact and settle from initial conditions. The very large PPMRs of salps, larvaceans and euphausiids means that simulated biomass does not settle to a constant level as the simulation progresses, an effect that has been observed in many theoretical studies^{16,96–98}. Rather, model biomass for the different groups settles into a series of repeating cycles through time. To address this, results are obtained by calculating mean diets and biomass over the last 500 years of each simulation for each functional group, to obtain long-term averages over the repeating cycles.

Assessing climate effects on zooplankton

We assess changes in the biomass of omnivores (euphausiids and omnivorous copepods), filter feeders (larvaceans and salps) and carnivores (chaetognaths, jellyfish and carnivorous copepods) as well as resultant changes in zooplankton community composition and implications for SPF, under three future (2015–2100) Intergovernmental Panel on Climate Change SSP scenarios¹⁹ (SSP 1–2.6, SSP 3–7.0 and SSP 5–8.5) using historical (1980–2000) conditions as a baseline. Environmental drivers required to run the model over the historical and three future SSP scenarios were sourced from five CMIP6 (ref. ²⁰) Earth-system models: CESM2, GFDL-ESM4, IPSL-CM6A-LR, MPI-ESM1-2-HR and UKESM1-0-LL. We chose these five models because they had been previously selected from the larger CMIP6 model cohort to force ecosystem models in the fisheries and marine ecosystem model intercomparison project (FishMIP), of which ZooMSS is a participating model (<https://www.isimip.org/protocol/3/>).

To assess climate effects across polar, westerlies (temperate) and trades (tropical) Longhurst biomes⁹⁹ (Extended Data Fig. 10), we used the Longhurst biome mask from <https://www.marinerregions.org>. Throughout this work, we have renamed the westerlies and trades biomes to temperate and tropical. Climate-driven changes in phytoplankton are highly uncertain, especially in coastal regions⁹⁰. This is because global Earth-system models with 1° spatial resolution—such as the five used in this study—do not properly resolve biogeochemical dynamics in coastal systems^{90,100–103}. For example, in the Peru upwelling, downscaled phytoplankton biomass from three different ESMs (CNRM, GFDL and IPSL) were compared with phytoplankton biomass from the same models but at their original (coarser) resolution¹⁰³. From 2005 to 2100 under representative concentration pathway (RCP) 8.5, the coarser resolution models predicted a decrease in chlorophyll (between –11% and –104%), whereas the higher resolution versions projected an increase of between 2% and 17%. Because of this uncertainty, we excluded the coastal Longhurst biome from our results.

Calculating fish diet, trophic level and diet carbon content

The trophic level of SPF (TL_{SPF}) was calculated for all fish with an asymptotic size of 100 g irrespective of life stage, which is because the trophic level of an individual is more related to its body size than life stage¹⁰⁴:

$$TL_{SPF} = 1 + \sum_j TL_j \times PD_{SPF,j},$$

where TL_{*j*} is the trophic level of group *j* and PD_{SPF,*j*} is the proportion of the diet of SPF from group *j*:

$$PD_{SPF,j} = \frac{F_{SPF,j}}{\sum_j F_{SPF,j}},$$

and *F*_{SPF,*j*} is the total biomass from group *j* consumed by SPF. Except for phytoplankton, which have a fixed trophic level of 1, the trophic levels of the different zooplankton and fish groups change with their diet, so we used the Gauss–Jacobi iteration method to solve TL_{SPF}.

SPF diet carbon content, CC_{SPF}, was:

$$CC_{SPF} = \frac{\sum_j C_j B_{SPF,j}}{\sum_j B_{SPF,j}},$$

where *B*_{SPF,*j*} is the total biomass from group *j* consumed by SPF and *C*_{*j*} is the carbon content of group *j*, as a proportion of total wet biomass.

Statistical methods

We ran ZooMSS five times in total, with each run forced by one of the five Earth-system models used. These simulations were summarized as means and standard deviations in figures and tables. To verify if mean changes in total zooplankton biomass and the biomass of filter feeders, carnivores and omnivores were significant, *P* values in Table 1 were calculated using two-sided Mann–Whitney non-parametric *U*-tests comparing initial (1980–2000, *n* = 100; 20 years × 5 simulations) and final (2080–2100, *n* = 100) biomass changes. Only biomass changes that had significant *P* values (*P* < 0.05) were discussed in the text.

Reporting summary

Further information on research design is available in the Nature Portfolio Reporting Summary linked to this article.

Data availability

ZooMSS environmental inputs were sourced from five climate models from CMIP6 (Methods; climate model data are available from the Earth System Grid Federation here: <https://esgf-data.dkrz.de/projects/esgf-dkrz/>). ZooMSS model outputs analysed in this study are available at <https://doi.org/10.5281/zenodo.7619220> (ref. ¹⁰⁵).

Code availability

ZooMSS model code is available at <https://github.com/MathMarEcol/ZoopModelSizeSpectra>. The code used to conduct all analysis in this study is available at <https://doi.org/10.5281/zenodo.7619220> (ref. ¹⁰⁵).

References

- Blanchard, J. L., Heneghan, R. F., Everett, J. D., Trebilco, R. & Richardson, A. J. From bacteria to whales: using functional size spectra to model marine ecosystems. *Trends Ecol. Evol.* **32**, 174–186 (2017).
- Strömberg, K. H. P., Smyth, T. J., Allen, J. I., Pitois, S. & O'Brien, T. D. Estimation of global zooplankton biomass from satellite ocean colour. *J. Mar. Syst.* **78**, 18–27 (2009).
- Hirst, A. G., Roff, J. C. & Lampitt, R. S. A synthesis of growth rates in marine epipelagic invertebrate zooplankton. *Adv. Marine Biol.* **44**, 1–142 (2003).

63. Clarke, A. *Principles of Thermal Ecology: Temperature, Energy, and Life* Vol. 1 (Oxford Univ. Press, 2017).
64. Brewin, R. J. W. et al. Influence of light in the mixed-layer on the parameters of a three-component model of phytoplankton size class. *Remote Sens. Environ.* **168**, 437–450 (2015).
65. Marañón, E. et al. Resource supply overrides temperature as a controlling factor of marine phytoplankton growth. *PLoS ONE* **9**, e99312 (2014).
66. Boudreau, P. R. & Dickie, L. M. Biomass spectra of aquatic ecosystems in relation to fisheries yield. *Can. J. Fish. Aquat. Sci.* **49**, 1528–1538 (1992).
67. Huete-Ortega, M., Cermeño, P., Calvo-Díaz, A. & Marañón, E. Isometric size-scaling of metabolic rate and the size abundance distribution of phytoplankton. *Proc. R. Soc. B* **279**, 1815–1823 (2012).
68. Marañón, E. Cell size as a key determinant of phytoplankton metabolism and community structure. *Annu. Rev. Mar. Sci.* **7**, 241–264 (2015).
69. Moreno-Ostos, E. et al. Phytoplankton biovolume is independent from the slope of the size spectrum in the oligotrophic Atlantic Ocean. *J. Mar. Syst.* **152**, 42–50 (2015).
70. Woodworth-Jefcoats, P. A., Polovina, J. J., Dunne, J. P. & Blanchard, J. L. Ecosystem size structure response to 21st century climate projection: large fish abundance decreases in the central North Pacific and increases in the California Current. *Glob. Change Biol.* **19**, 724–733 (2013).
71. Cullen, J. J. Subsurface chlorophyll maximum layers: enduring enigma or mystery solved? *Annu. Rev. Mar. Sci.* **7**, 207–239 (2015).
72. Barnes, C., Irigoien, X., De Oliveira, J. A. A., Maxwell, D. & Jennings, S. Predicting marine phytoplankton community size structure from empirical relationships with remotely sensed variables. *J. Plankton Res.* **33**, 13–24 (2011).
73. Hirata, T. et al. Synoptic relationships between surface chlorophyll-a and diagnostic pigments specific to phytoplankton functional types. *Biogeosciences* **8**, 311–327 (2011).
74. Uitz, J., Claustre, H., Morel, A. & Hooker, S. B. Vertical distribution of phytoplankton communities in open ocean: an assessment based on surface chlorophyll. *J. Geophys. Res.* **111**, C08005 (2006).
75. Asghar, U. et al. Morphogenesis of the ciliature during sexual process of conjugation in the ciliated protist *Euplotes raikovi*. *Front. Mar. Sci.* **7**, 615377 (2021).
76. Pecková, H. & Lom, J. Growth, morphology and division of flagellates of the genus *Trypanoplasma* (Protozoa, Kinetoplastida) in vitro. *Parasitol. Res.* **76**, 553–558 (1990).
77. Daponte, M. C., Palmieri, M. A., Casareto, B. E. & Esnal, G. B. Reproduction and population structure of the salp *Lasis zonaria* (Pallas, 1774) in the southwestern Atlantic Ocean (34°30' to 39°30'S) during three successive winters (1999–2001). *J. Plankton Res.* **35**, 813–830 (2013).
78. Fautin, D. G. Reproduction of Cnidaria. *Can. J. Zool.* **80**, 1735–1754 (2002).
79. Bone, Q. et al. *The Biology of Chaetognaths* (Oxford Univ. Press, 1991).
80. Gusmao, L. F. M. & McKinnon, A. D. Sex ratios, intersexuality and sex change in copepods. *J. Plankton Res.* **31**, 1101–1117 (2009).
81. Falkowski, P. G. et al. The fate of a spring phytoplankton bloom: export or oxidation? *Cont. Shelf Res.* **8**, 457–484 (1988).
82. Atkinson, A. et al. Zooplankton response to a phytoplankton bloom near South Georgia, Antarctica. *Mar. Ecol. Prog. Ser.* **144**, 195–210 (1996).
83. Blanchard, J. L. et al. How does abundance scale with body size in coupled size-structured food webs? *J. Anim. Ecol.* **78**, 270–280 (2009).
84. *Phytoplankton Functional Types from Space* (IOCCG, 2014); <https://doi.org/10.25607/OBP-106>
85. Padfield, D., Yvon-Durocher, G., Buckling, A., Jennings, S. & Yvon-Durocher, G. Rapid evolution of metabolic traits explains thermal adaptation in phytoplankton. *Ecol. Lett.* **19**, 133–142 (2016).
86. Peter, K. H. & Sommer, U. Phytoplankton cell size reduction in response to warming mediated by nutrient limitation. *PLoS ONE* **8**, e71528 (2013).
87. Flombaum, P., Wang, W.-L., Primeau, F. W. & Martiny, A. C. Global picophytoplankton niche partitioning predicts overall positive response to ocean warming. *Nat. Geosci.* **13**, 116–120 (2020).
88. Polovina, J. J., Howell, E. A. & Abecassis, M. Ocean's least productive waters are expanding. *Geophys. Res. Lett.* **35**, L03618 (2008).
89. Kjørboe, T. & Hirst, A. G. Shifts in mass scaling of respiration, feeding, and growth rates across life-form transitions in marine pelagic organisms. *Am. Nat.* **183**, E118–E130 (2014).
90. Kearney, K. A. et al. Using global-scale Earth system models for regional fisheries applications. *Front. Mar. Sci.* **8**, 622206 (2021).
91. Blanchard, J. L. et al. Potential consequences of climate change for primary production and fish production in large marine ecosystems. *Philos. Trans. R. Soc. B* **367**, 2979–2989 (2012).
92. Carozza, D. A., Bianchi, D. & Galbraith, E. D. The ecological module of BOATS-1.0: a bioenergetically constrained model of marine upper trophic levels suitable for studies of fisheries and ocean biogeochemistry. *Geosci. Model Dev.* **9**, 1545–1565 (2016).
93. Petrik, C. M., Stock, C. A., Andersen, K. H., van Denderen, P. D. & Watson, J. R. Bottom-up drivers of global patterns of demersal, forage, and pelagic fishes. *Prog. Oceanogr.* **176**, 102124 (2019).
94. Pontavice, H., Gascuel, D., Reygondeau, G., Stock, C. & Cheung, W. W. L. Climate-induced decrease in biomass flow in marine food webs may severely affect predators and ecosystem production. *Glob. Change Biol.* **27**, 2608–2622 (2021).
95. *Numerical Recipes: The Art of Scientific Computing* (Cambridge Univ. Press, 2007).
96. Law, R., Plank, M. J., James, A. & Blanchard, J. L. Size-spectra dynamics from stochastic predation and growth of individuals. *Ecology* **90**, 802–811 (2009).
97. Datta, S., Delius, G. W., Law, R. & Plank, M. J. A stability analysis of the power-law steady state of marine size spectra. *J. Math. Biol.* **63**, 779–799 (2011).
98. Plank, M. J. & Law, R. Ecological drivers of stability and instability in marine ecosystems. *Theor. Ecol.* **5**, 465–480 (2012).
99. Longhurst, A. R. *Ecological Geography of the Sea* (Academic Press, 2007).
100. Holt, J. et al. Modelling the global coastal ocean. *Philos. Trans. R. Soc. A* **367**, 939–951 (2009).
101. Asch, R. G., Holding, J. M., Pilcher, D. J., Rivero-Calle, S. & Rose, K. A. Editorial: Ecological applications of Earth system models and regional climate models. *Front. Mar. Sci.* **8**, 773443 (2021).
102. Drenkard, E. J. et al. Next-generation regional ocean projections for living marine resource management in a changing climate. *ICES J. Mar. Sci.* **78**, 1969–1987 (2021).
103. Echevin, V. et al. Physical and biogeochemical impacts of RCP8.5 scenario in the Peru upwelling system. *Biogeosciences* **17**, 3317–3341 (2020).
104. Andersen, K. H. et al. Characteristic sizes of life in the oceans, from bacteria to whales. *Annu. Rev. Mar. Sci.* **8**, 217–241 (2016).
105. Heneghan, R. F. et al. Data and code for 'Climate-driven zooplankton shifts cause large-scale declines in food quality for fish'. Zenodo <https://doi.org/10.5281/zenodo.7619220> (2023).

Acknowledgements

P.S. was supported by an Australian Government Research Training Program Scholarship. J.D.E. was funded by Australian Research Council Discovery Projects DP150102656 and DP190102293.

Author contributions

R.F.H., A.J.R. and J.D.E. defined the research question for this study. J.D.E. conducted the simulations, with the assistance from R.F.H. R.F.H. drafted the manuscript, with the assistance and feedback from A.J.R., J.D.E., P.S. and J.L.B.

Competing interests

The authors declare no competing interests.

Additional information

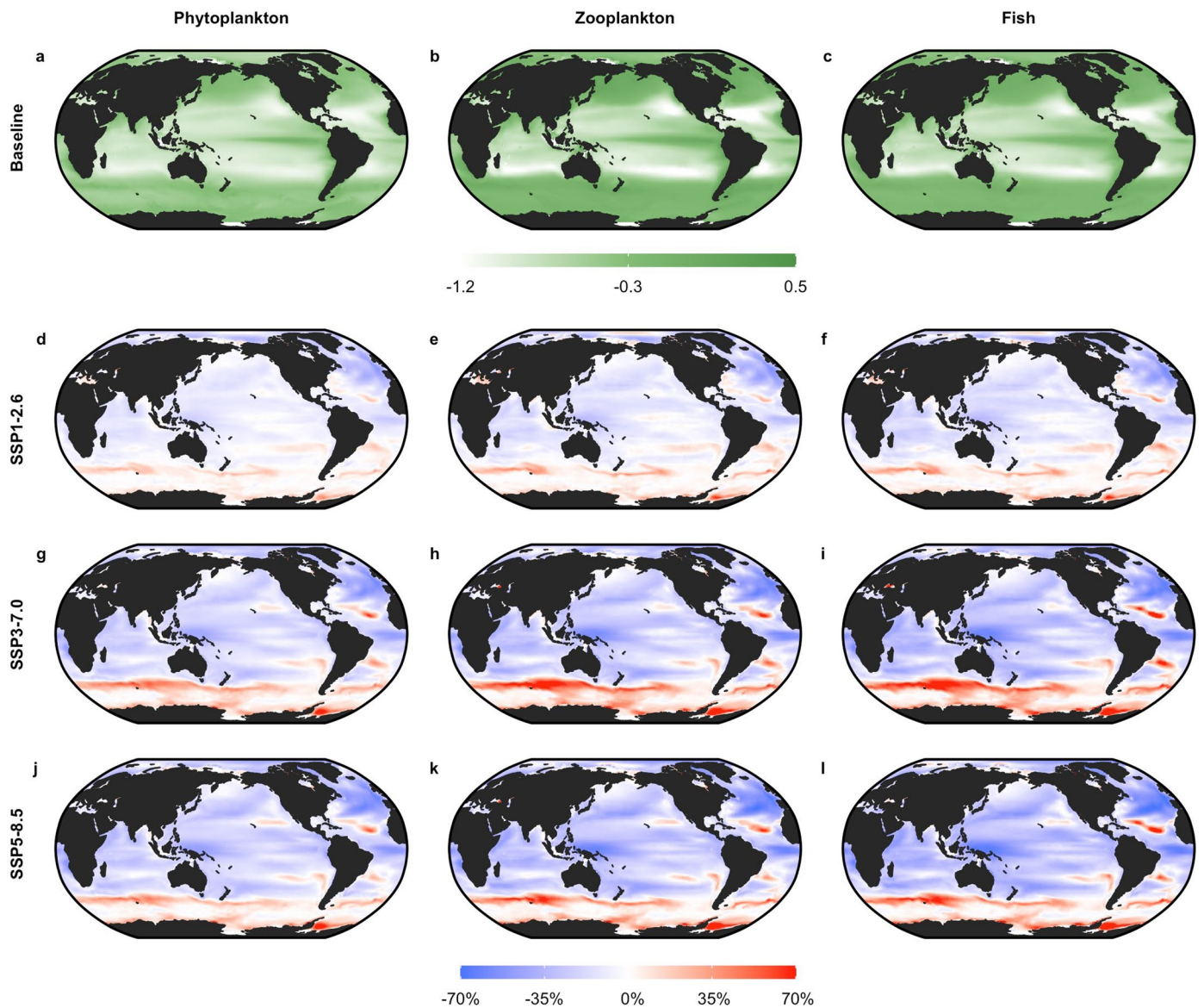
Extended data is available for this paper at <https://doi.org/10.1038/s41558-023-01630-7>.

Supplementary information The online version contains supplementary material available at <https://doi.org/10.1038/s41558-023-01630-7>.

Correspondence and requests for materials should be addressed to Ryan F. Heneghan.

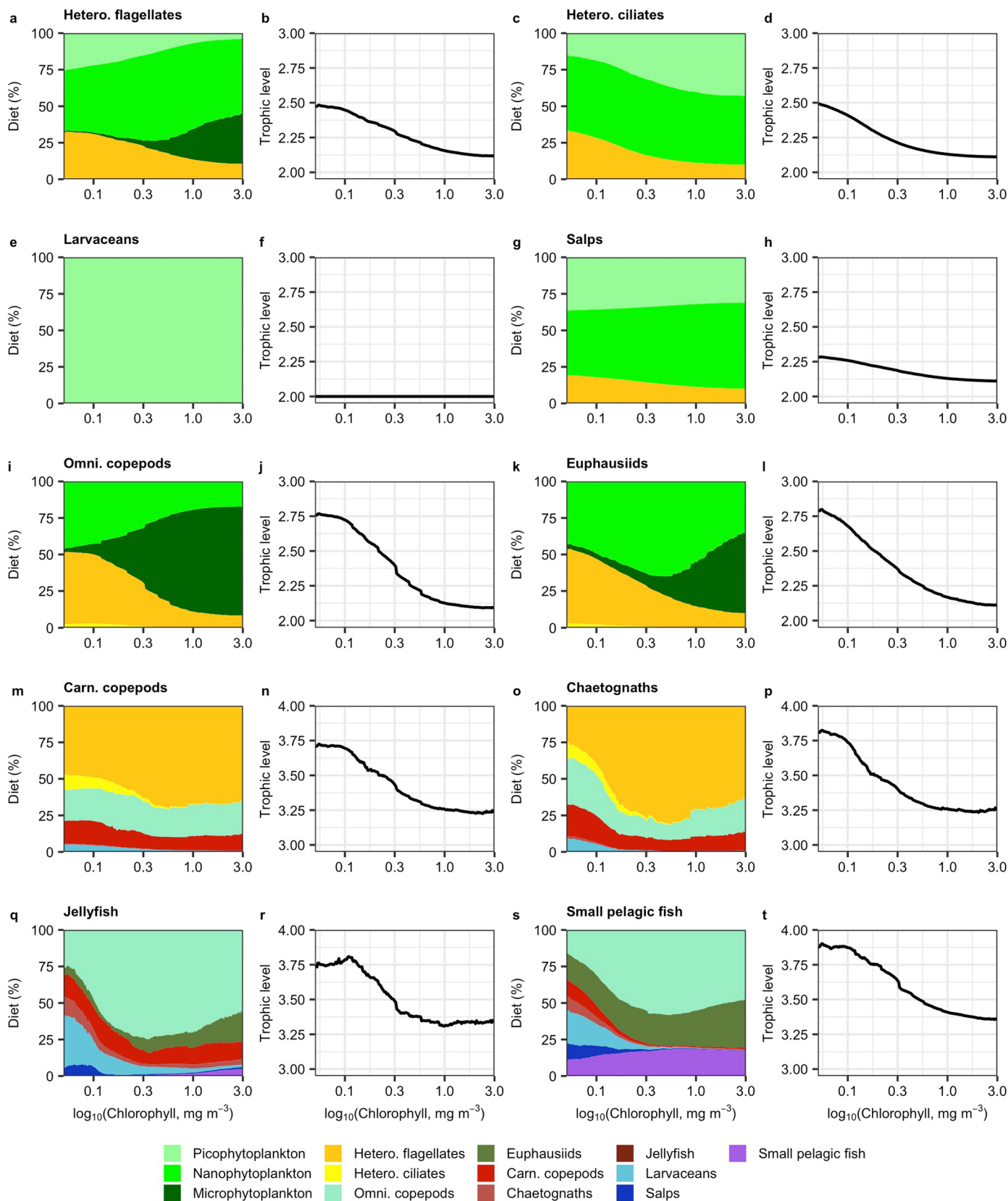
Peer review information *Nature Climate Change* thanks Melika Baklouti, Fabien Lombard, Rebecca Wright and the other, anonymous, reviewer(s) for their contribution to the peer review of this work.

Reprints and permissions information is available at www.nature.com/reprints.



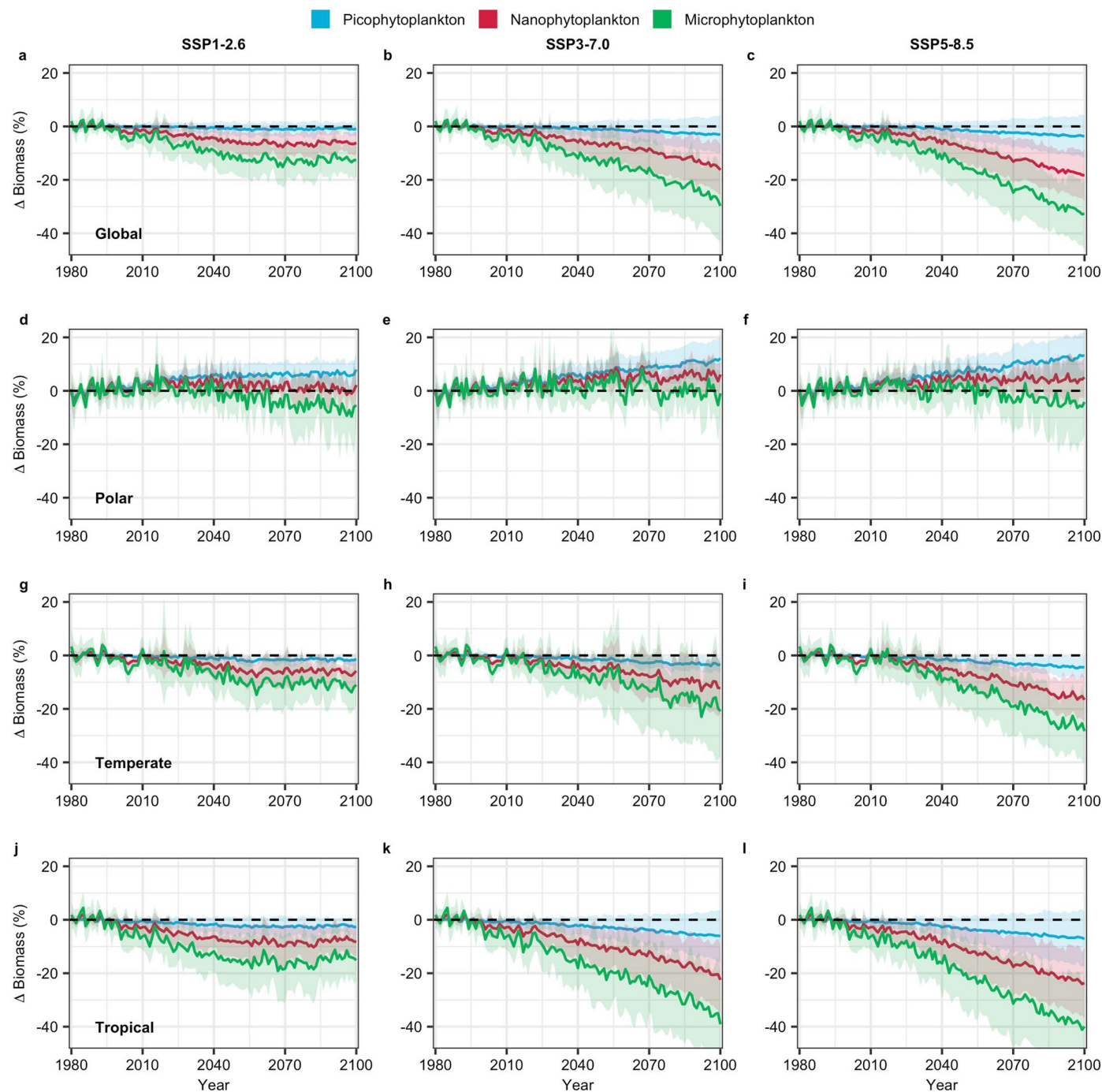
Extended Data Fig. 1 | Climate-induced shifts in biomass of phytoplankton, zooplankton and SPF. Mean \log_{10} biomass (g m^{-2}) in 1980–2000 of: **a**, Phytoplankton; **b**, Zooplankton (both micro and macrozooplankton); **c**, SPF; **(d–l)**, Maps of the mean change in the total biomass of: **(d, g, j)**, Phytoplankton; **(e, h, k)**, Zooplankton; and **(f, i, l)**, SPF in 2080–2100 compared with 1980–2000

under emission scenarios SSP1–2.6 **(d–f)**, SSP3–7.0 **(g–i)** and SSP5–8.5 **(j–l)**, across the five Earth-system models used to force ZooMSS (see Assessing climate impacts on zooplankton in Methods for more information about Earth-system models used in this study).



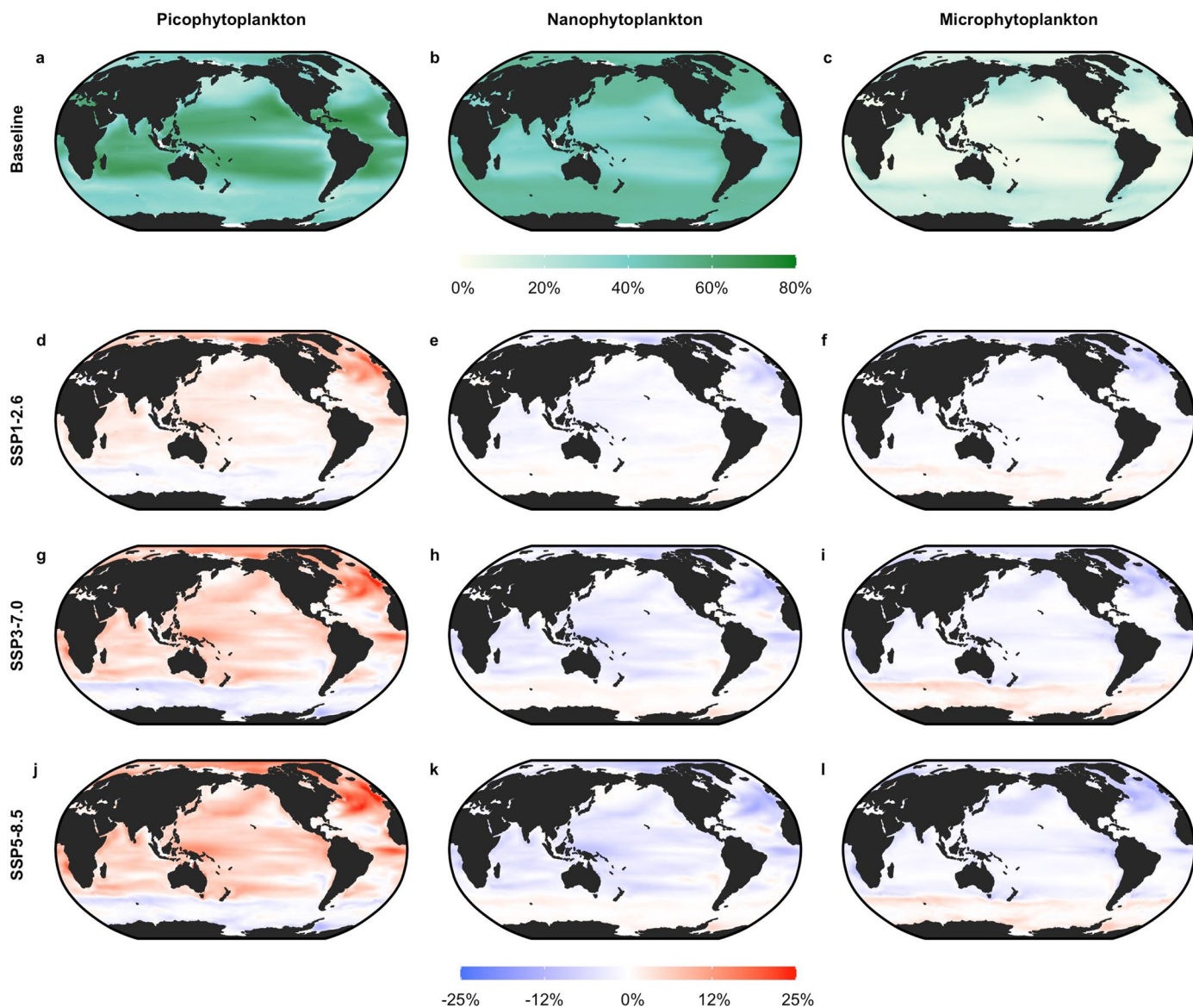
Extended Data Fig. 2 | Diet composition and trophic level of the 9 zooplankton groups in ZoomSS. Mean diet composition and resultant trophic level across the global chlorophyll gradient from the five Earth-system models used to force ZoomSS for **a, b**, Heterotrophic (Hetero.) flagellates;

c, d, Heterotrophic (Hetero.) ciliates; **e, f**, Larvaceans; **g, h**, Salps; **i, j**, Omnivorous (Omni.) copepods; **k, l**, Euphausiids; **m, n**, Carnivorous (Carn.) copepods; **o, p**, Chaetognaths; **q, r**, Jellyfish; **s, t**, SPF.



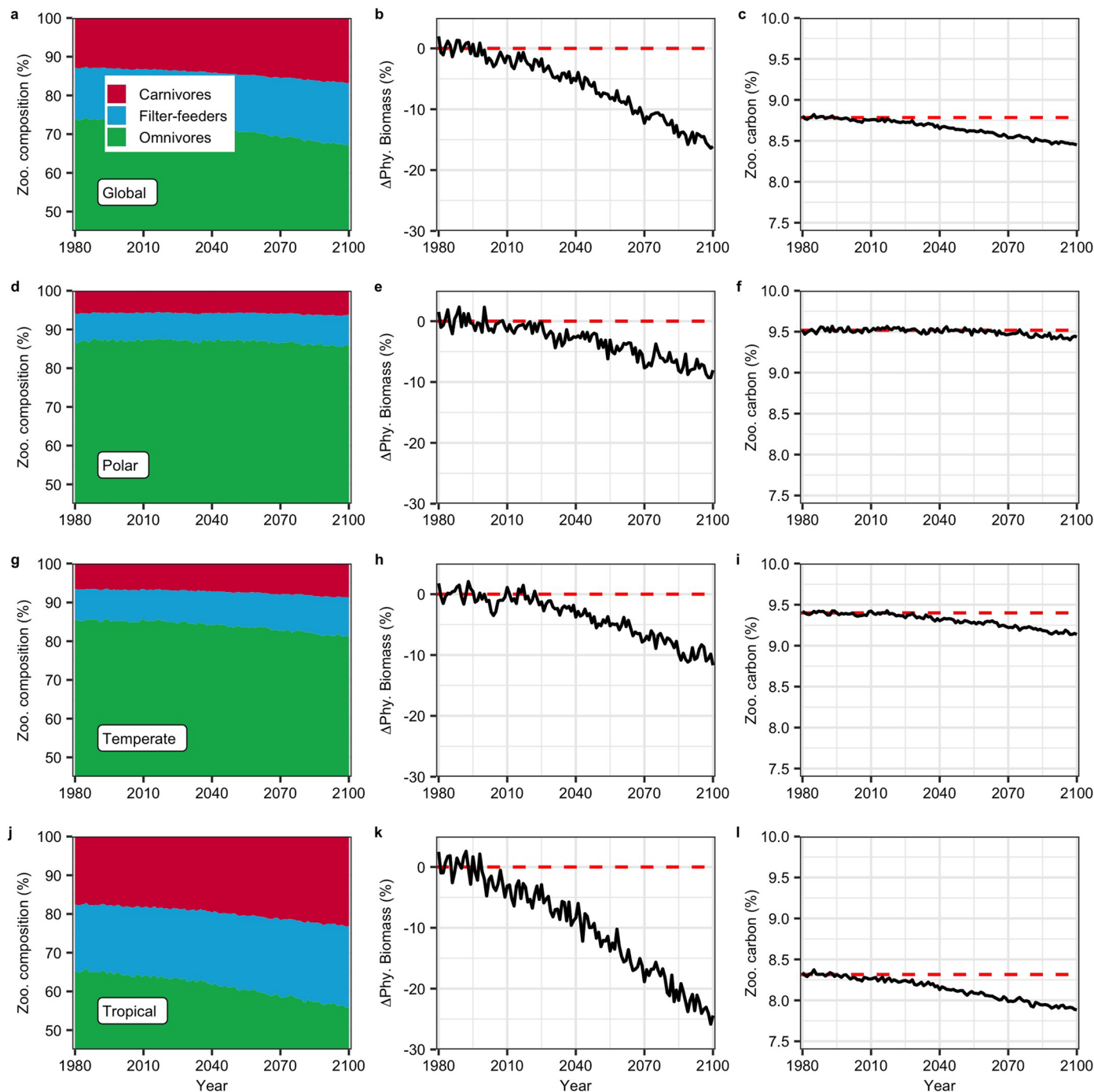
Extended Data Fig. 3 | Impacts of climate change on the three phytoplankton groups. Change in global biomass (%) for the three phytoplankton groups (Picophytoplankton, 0.2–2 μm ESD; Nanophytoplankton, 2–20 μm ESD; Microphytoplankton, >20 μm ESD) from 1980–2100, relative to 1980–2000, under emission scenarios (a, d, g, j) SSP1–2.6; (b, e, h, k) SSP3–7.0; and (c, f, i, l) SSP5–8.5, across (a–c) Global; (d–f) Polar; (g–i) Temperate; and (j–l) Tropical waters. Note here that Temperate and Tropical respectively correspond to

Westerlies and Trades Longhurst biomes, and Global results exclude the Coastal biome, see Extended Data Figure 10 for a map of the biomes. Solid lines give the ensemble mean change and shaded areas represent the standard deviation for each phytoplankton group across the five Earth-system models used to provide forcings for ZooMSS. The dashed black line in each plot represents no change from mean biomass in 1980–2000.



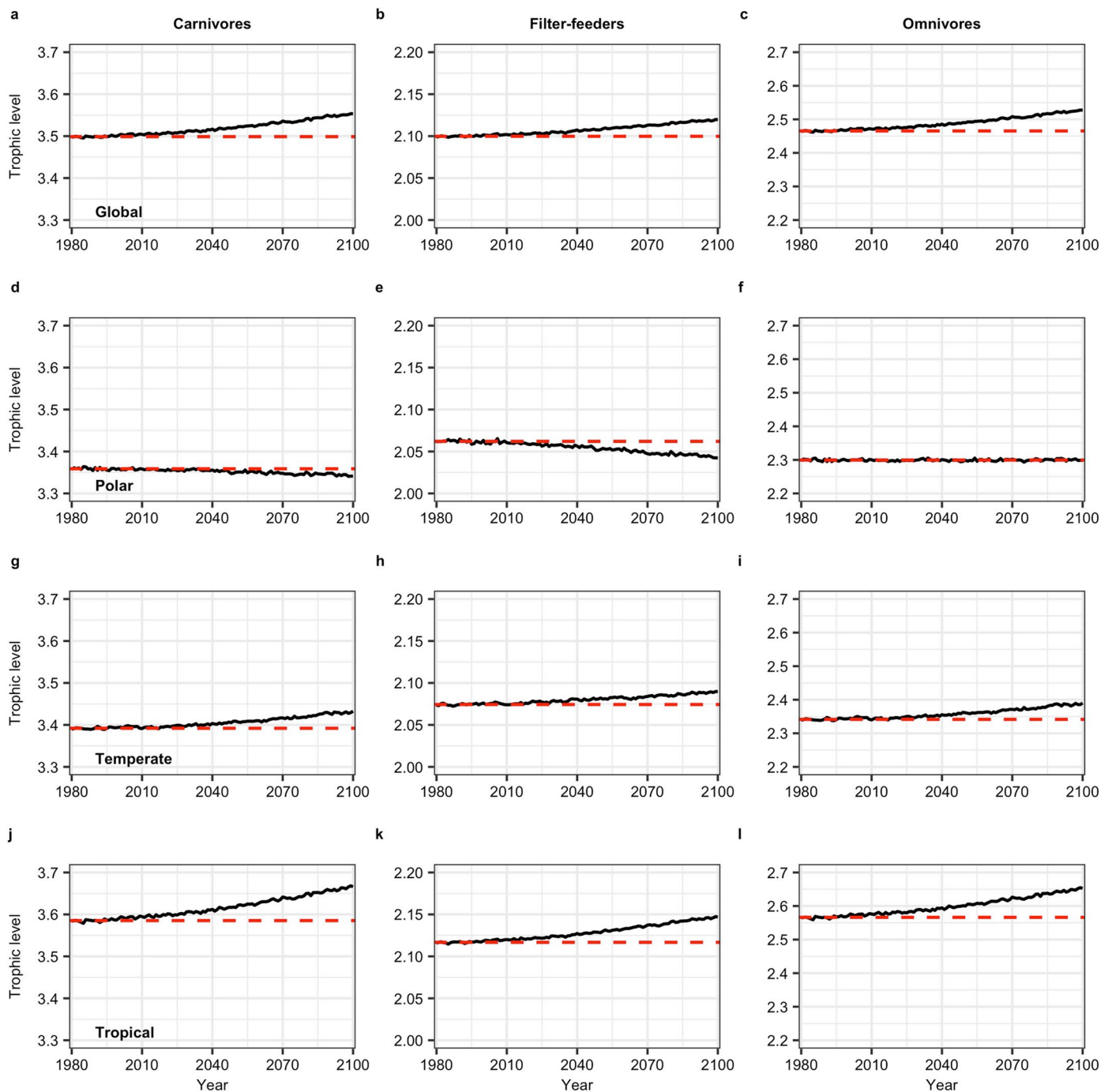
Extended Data Fig. 4 | Climate-induced shifts in biomass of pico (0.2–2 μm ESD), nano (2–20 μm ESD) and microphytoplankton (>20 μm ESD). The baseline percentage of total phytoplankton biomass in 1980–2000 comprising: **a**, Picophytoplankton; **b**, Nanophytoplankton; **c**, Microphytoplankton. **d–l**, Maps of the mean change (%) of total phytoplankton biomass from:

(d, g, j) Picophytoplankton; **(e, h, k)** Nanophytoplankton; and **(f, i, l)** Microphytoplankton in 2080–2100 relative to 1980–2000 under emission scenarios **(d–f)** SSP 1–2.6; **(g–i)** SSP 3–7.0; and **(j–l)** SSP 5–8.5, across the five Earth-system models used to force ZooMSS.



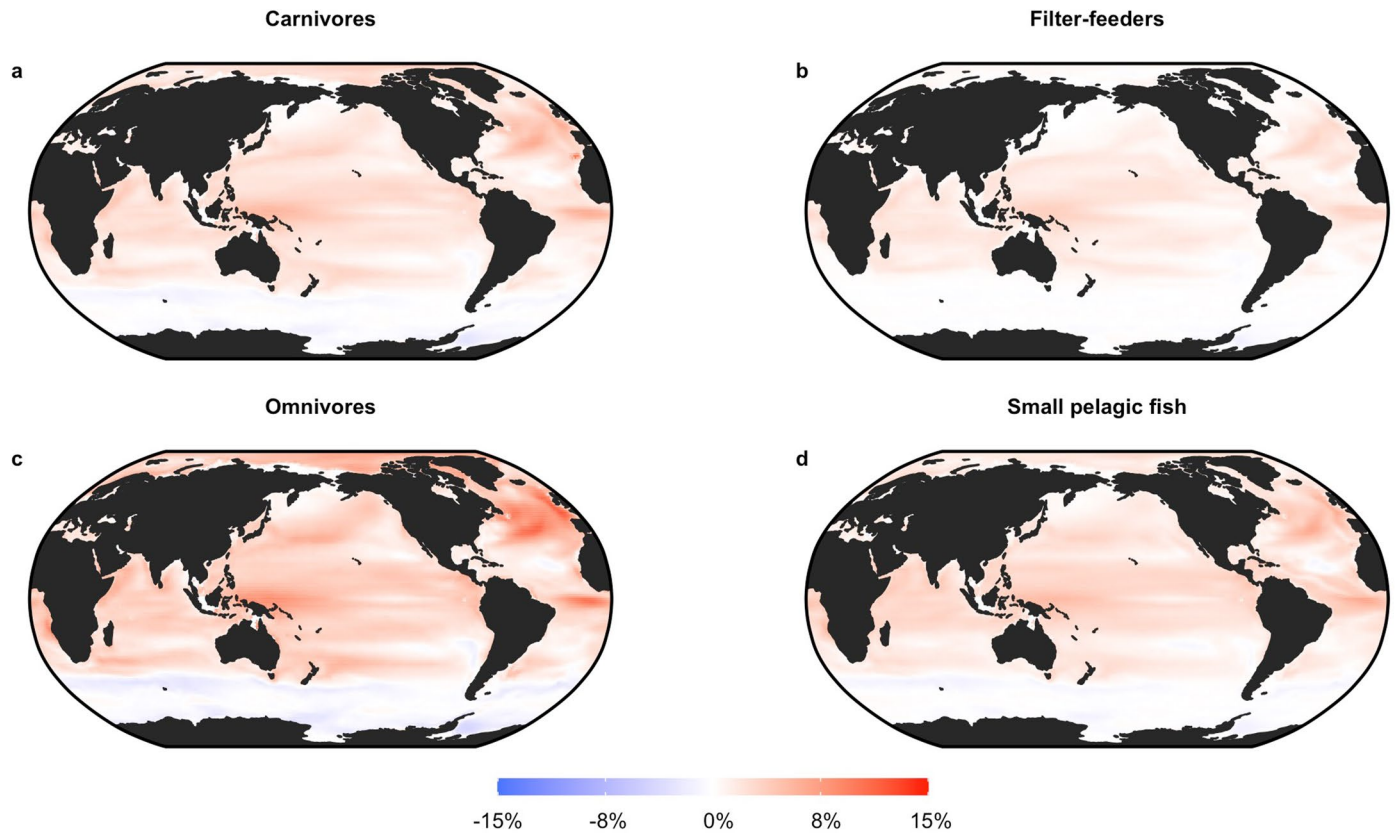
Extended Data Fig. 5 | Impacts of climate change on the plankton. Mean change (%) in (a, d, g, j) zooplankton (Zoo.) community composition; (b, e, h, k) phytoplankton (Phy.) biomass and (c, f, i, l) zooplankton community carbon content (Zoo. carbon), relative to 1980–2000 under SSP 5–8.5, in (a–c) Global; (d–f) Polar; (g–i) Temperate and (j–l) Tropical waters, across the five Earth-system models used to force ZooMSS in this study. Carnivores include

chaetognaths, jellyfish and carnivorous copepods, Filter-feeders include salps and larvaceans, and Omnivores include euphausiids and omnivorous copepods. Note here that Temperate and Tropical respectively correspond to Westerlies and Trades Longhurst biomes, and Global results exclude the Coastal biome, see Extended Data Figure 10 for a map of the biomes.

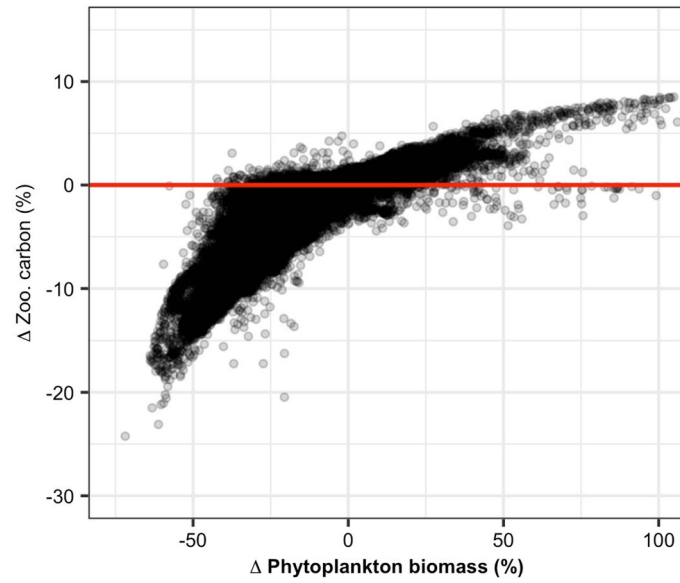


Extended Data Fig. 6 | Impacts of climate change on zooplankton trophic levels. Mean trophic level of carnivores (carnivorous copepods, chaetognaths and jellyfish; **a, d, g, j**), filter-feeders (salps and larvaceans; **b, e, h, k**) and omnivores (omnivorous copepods and euphausiids; **c, f, i, l**) from 1980–2100 under SSP 5–8.5 in (**a–c**) Global; (**d–f**) Polar; (**g–i**) Temperate and (**j–l**) Tropical

waters, across the five Earth-system models used to force ZooMSS in this study. Note here that Temperate and Tropical respectively correspond to Westerlies and Trades Longhurst biomes, and Global results exclude the Coastal biome, see Extended Data Figure 10 for a map of the biomes. The red dashed line in each figure indicates the mean trophic level from 1980–2000.

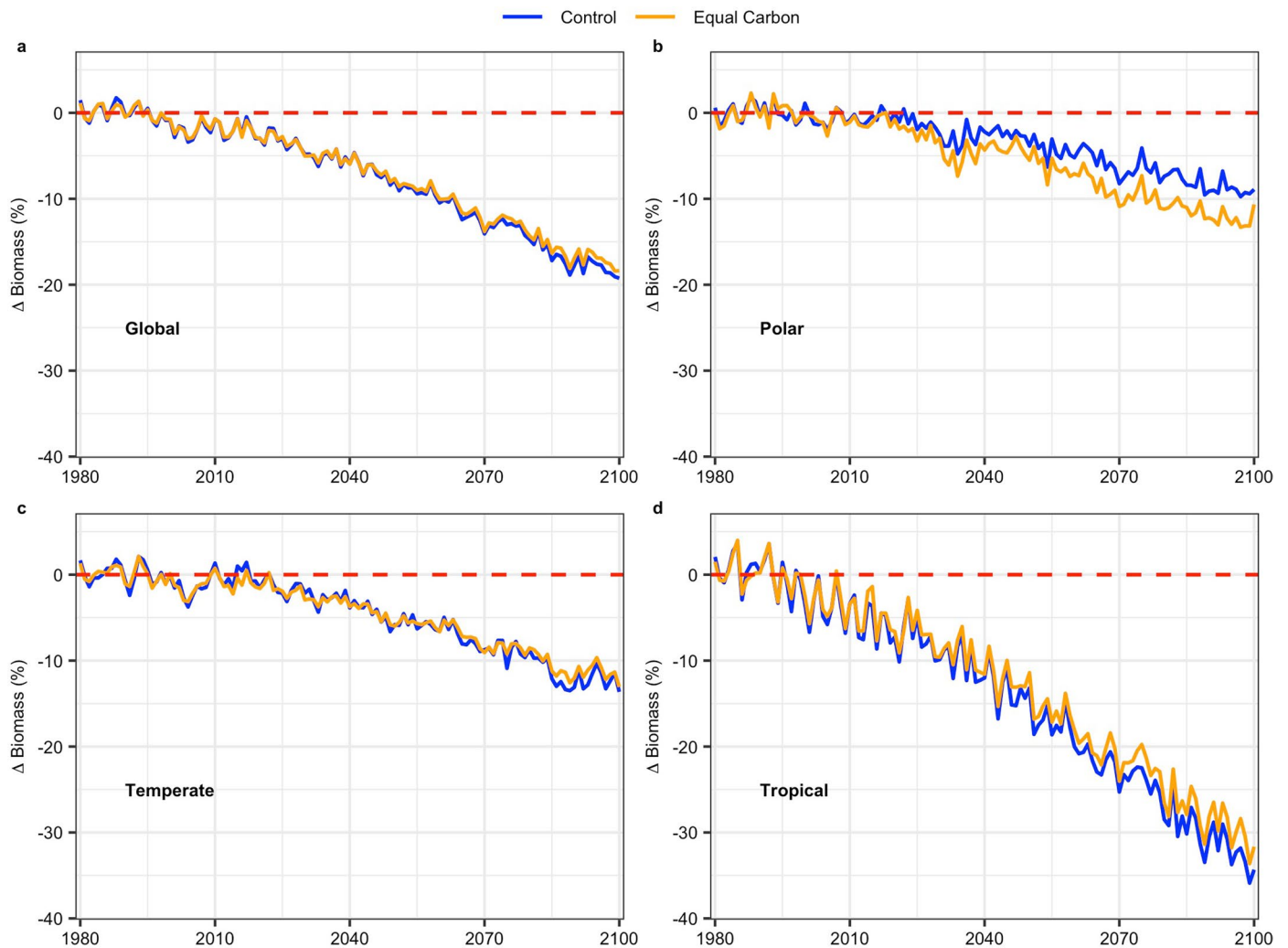


Extended Data Fig. 7 | Climate-induced shifts in trophic levels. Maps of the mean change (%) in trophic level of **a**, Carnivores; **b**, Filter-feeders; **c**, Omnivores; and **d**, Small (Pelagic) fish in 2080–2100 relative to 1980–2000 under emission scenarios SSP 5–8.5, across the five Earth-system models used to force ZooMSS.



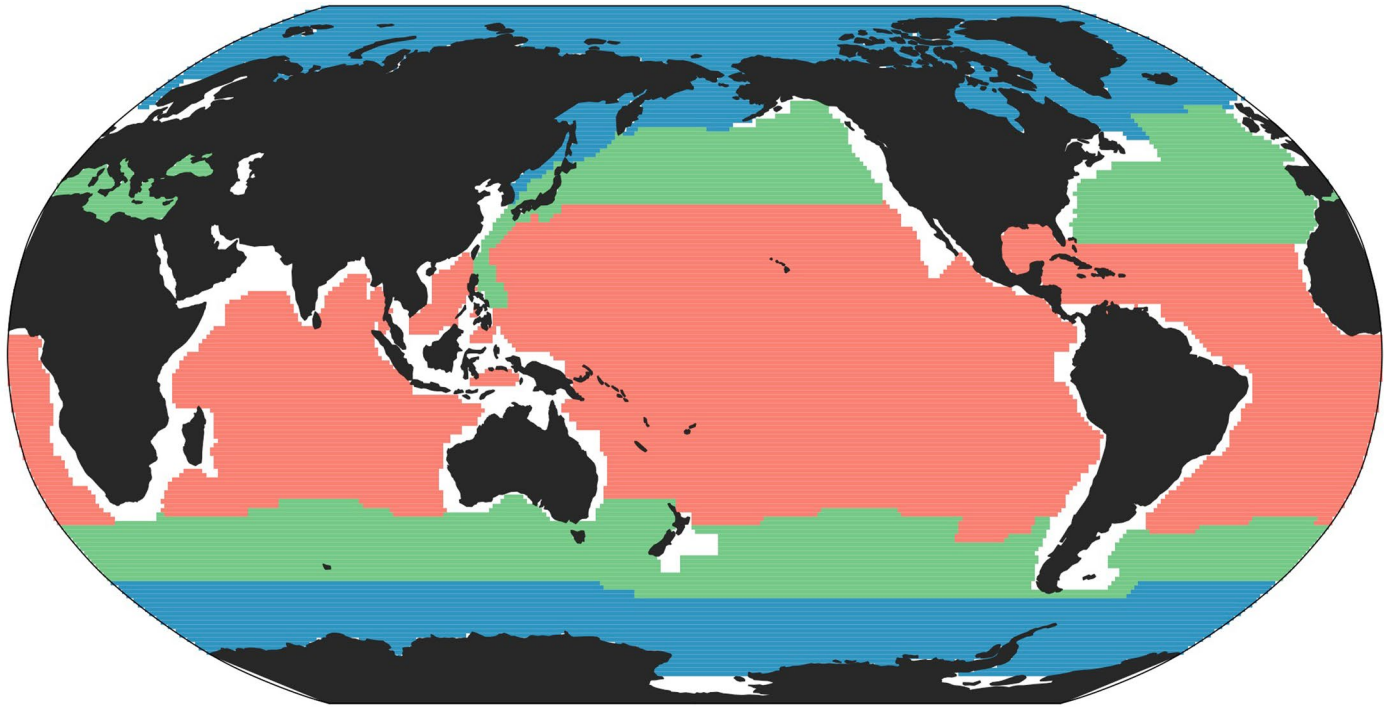
Extended Data Fig. 8 | Impacts of changing phytoplankton biomass on zooplankton community carbon content. Percentage change in zooplankton community carbon content against the percentage change in phytoplankton

biomass, for individual 1° grid squares from 1980–2000 to 2080–2100 under the SSP 5–8.5 emissions scenario. The red solid horizontal line indicates where the percentage change in zooplankton community carbon content is zero.



Extended Data Fig. 9 | Impacts of zooplankton carbon content on SPF biomass. Mean percentage change in the biomass of SPF under SSP 5–8.5, from 1980–2100 across **a**, Global (excluding the coastal biome); **b**, Polar; **c**, Temperate; **d**, Tropical waters. The blue line in each plot is the change in small pelagic biomass under the standard model run, where the carbon content of each

zooplankton group is given in Table S1, while the orange line is the change in SPF biomass when the carbon content of all zooplankton groups is fixed at 10%. The red dashed line indicates where there is no biomass change against mean levels in 1980–2000.



■ Polar ■ Temperate ■ Tropical

Extended Data Fig. 10 | Map of the three Longhurst ocean biomes used in this study. The Coastal biome has been excluded from our analysis. Note that in this study, the Westerlies and Trades biomes have been renamed to Temperate and Tropical, respectively. See Assessing climate impacts on zooplankton in the Methods for more information.

Reporting Summary

Nature Portfolio wishes to improve the reproducibility of the work that we publish. This form provides structure for consistency and transparency in reporting. For further information on Nature Portfolio policies, see our [Editorial Policies](#) and the [Editorial Policy Checklist](#).

Statistics

For all statistical analyses, confirm that the following items are present in the figure legend, table legend, main text, or Methods section.

n/a Confirmed

- The exact sample size (n) for each experimental group/condition, given as a discrete number and unit of measurement
- A statement on whether measurements were taken from distinct samples or whether the same sample was measured repeatedly
- The statistical test(s) used AND whether they are one- or two-sided
Only common tests should be described solely by name; describe more complex techniques in the Methods section.
- A description of all covariates tested
- A description of any assumptions or corrections, such as tests of normality and adjustment for multiple comparisons
- A full description of the statistical parameters including central tendency (e.g. means) or other basic estimates (e.g. regression coefficient) AND variation (e.g. standard deviation) or associated estimates of uncertainty (e.g. confidence intervals)
- For null hypothesis testing, the test statistic (e.g. F , t , r) with confidence intervals, effect sizes, degrees of freedom and P value noted
Give P values as exact values whenever suitable.
- For Bayesian analysis, information on the choice of priors and Markov chain Monte Carlo settings
- For hierarchical and complex designs, identification of the appropriate level for tests and full reporting of outcomes
- Estimates of effect sizes (e.g. Cohen's d , Pearson's r), indicating how they were calculated

Our web collection on [statistics for biologists](#) contains articles on many of the points above.

Software and code

Policy information about [availability of computer code](#)

Data collection

Data was collected using the Zooplankton Model of Size Spectra (ZooMSS). Code to run ZooMSS is available here: <https://github.com/MathMarEcol/ZoopModelSizeSpectra>. ZooMSS model outputs analysed in this study are available at <https://doi.org/10.5281/zenodo.7619220>. All other inputs to force ZooMSS came from existing sources (see 'Assessing climate impacts on zooplankton' in Methods section).

Data analysis

We used CDO (climate data operators) and R 4.2.2 to analyse the data in this study. All code and data used to generate results in this study are available at Zenodo: <https://doi.org/10.5281/zenodo.7619220>

For manuscripts utilizing custom algorithms or software that are central to the research but not yet described in published literature, software must be made available to editors and reviewers. We strongly encourage code deposition in a community repository (e.g. GitHub). See the Nature Portfolio [guidelines for submitting code & software](#) for further information.

Data

Policy information about [availability of data](#)

All manuscripts must include a [data availability statement](#). This statement should provide the following information, where applicable:

- Accession codes, unique identifiers, or web links for publicly available datasets
- A description of any restrictions on data availability
- For clinical datasets or third party data, please ensure that the statement adheres to our [policy](#)

ZooMSS environmental inputs were sourced from five climate models from CMIP6 (see Methods for more information; climate model data are available here: <https://esgf-node.llnl.gov/search/cmip6/>). ZooMSS model outputs analysed in this study are available at <https://doi.org/10.5281/zenodo.7619220>

Human research participants

Policy information about [studies involving human research participants and Sex and Gender in Research](#).

Reporting on sex and gender	N/A
Population characteristics	N/A
Recruitment	N/A
Ethics oversight	N/A

Note that full information on the approval of the study protocol must also be provided in the manuscript.

Field-specific reporting

Please select the one below that is the best fit for your research. If you are not sure, read the appropriate sections before making your selection.

- Life sciences Behavioural & social sciences Ecological, evolutionary & environmental sciences

For a reference copy of the document with all sections, see [nature.com/documents/nr-reporting-summary-flat.pdf](https://www.nature.com/documents/nr-reporting-summary-flat.pdf)

Ecological, evolutionary & environmental sciences study design

All studies must disclose on these points even when the disclosure is negative.

Study description	We used a global marine size-spectrum model (ZooMSS) to assess the impacts of climate change on the composition of zooplankton across the world's oceans. We also assessed potential implications for fish communities of projected changes in zooplankton composition.
Research sample	We used data on: Climate models: 5 earth-system models from the Coupled Model Intercomparison Project Phase 6 (https://esgf-node.llnl.gov/search/cmip6/) provided environmental forcings to force ZooMSS, from 1980-2100 under three climate change scenarios (SSP1-2.6, SSP3-7.0 and SSP5-8.5). The five models were CESM2, GFDL-ESM4, IPSL-CM6A-LR, MPI-ESM1-2-HR, UKESM1-0-LL. All models provided sea surface temperature and chlorophyll concentration. GFDL and CESM2 provided depth-resolved, size-fractionated phytoplankton carbon as well. Marine provinces: Longhurst biomes from Marine Regions (www.marineregions.org). This dataset has been provided in the Zenodo repository for this study).
Sampling strategy	Environmental drivers required to run the model over the historical and three future SSP scenarios were sourced from five Coupled Model Intercomparison Project Phase 620 (CMIP6) earth-system models: CESM2, GFDL-ESM4, IPSL-CM6A-LR, MPI-ESM1-2-HR, UKESM1-0-LL. We chose these five models because they had been previously selected from the larger CMIP6 model cohort to force ecosystem models in the Fisheries and marine ecosystem Model Intercomparison Project (FishMIP), of which ZooMSS is a participating model (https://www.isimip.org/protocol/3/).
Data collection	Data was generated by ZooMSS, or obtained from online repositories. All data presented in this study can be found at: https://doi.org/10.5281/zenodo.7619220
Timing and spatial scale	Global spatial scale, exploring 1980-2100 under three climate change scenarios (SSP1-2.6, SS3-7.0 and SSP5-8.5).
Data exclusions	No data were excluded from our study
Reproducibility	N/A - No experiments were performed

Randomization

N/A - No experiments were performed

Blinding

N/A - No experiments were performed

Did the study involve field work?

Yes

No

Reporting for specific materials, systems and methods

We require information from authors about some types of materials, experimental systems and methods used in many studies. Here, indicate whether each material, system or method listed is relevant to your study. If you are not sure if a list item applies to your research, read the appropriate section before selecting a response.

Materials & experimental systems

- | n/a | Involvement in the study |
|-------------------------------------|--|
| <input checked="" type="checkbox"/> | <input type="checkbox"/> Antibodies |
| <input checked="" type="checkbox"/> | <input type="checkbox"/> Eukaryotic cell lines |
| <input checked="" type="checkbox"/> | <input type="checkbox"/> Palaeontology and archaeology |
| <input checked="" type="checkbox"/> | <input type="checkbox"/> Animals and other organisms |
| <input checked="" type="checkbox"/> | <input type="checkbox"/> Clinical data |
| <input checked="" type="checkbox"/> | <input type="checkbox"/> Dual use research of concern |

Methods

- | n/a | Involvement in the study |
|-------------------------------------|---|
| <input checked="" type="checkbox"/> | <input type="checkbox"/> ChIP-seq |
| <input checked="" type="checkbox"/> | <input type="checkbox"/> Flow cytometry |
| <input checked="" type="checkbox"/> | <input type="checkbox"/> MRI-based neuroimaging |